

Spring 2018

Characterizing the Role of CP1 in *Drosophila Melanogaster*: Its Effects on Basement Membrane Degradation and Signaling

Dane Alan Flinchum

Western Kentucky University, dane.flinchum269@topper.wku.edu

Follow this and additional works at: <https://digitalcommons.wku.edu/theses>

 Part of the [Biology Commons](#), [Cell and Developmental Biology Commons](#), and the [Molecular Genetics Commons](#)

Recommended Citation

Flinchum, Dane Alan, "Characterizing the Role of CP1 in *Drosophila Melanogaster*: Its Effects on Basement Membrane Degradation and Signaling" (2018). *Masters Theses & Specialist Projects*. Paper 2642.
<https://digitalcommons.wku.edu/theses/2642>

This Thesis is brought to you for free and open access by TopSCHOLAR®. It has been accepted for inclusion in Masters Theses & Specialist Projects by an authorized administrator of TopSCHOLAR®. For more information, please contact topscholar@wku.edu.

CHARACTERIZING THE ROLE OF CP1 IN *DROSOPHILA MELANOGASTER*:
ITS EFFECTS ON BASEMENT MEMBRANE DEGRADATION AND SIGNALING

A Thesis
Presented to
The Faculty of the Department of Biology
Western Kentucky University
Bowling Green, Kentucky


In Partial Fulfillment
Of the Requirements for the Degree
Master of Science

By
Dane Alan Flinchum

May 2018

CHARACTERIZING THE ROLE OF CP1 IN *DROSOPHILA MELANOGASTER*:
ITS EFFECTS ON BASEMENT MEMBRANE DEGRADATION AND SIGNALING

Date Recommended 4/6/18


Ajay Srivastava, Ph.D. Thesis Director


Claire Rinehart, Ph. D.


Rodney King, Ph.D.


Dean, Graduate School

4/23/18
Date

This thesis would not have been possible without the support of many individuals. My parents, Gwen and Mark, who have loved and encouraged me through all of my endeavors. My brother Conor, who has always been there for me. The faculty, staff, and Biograds at WKU who have supported me during my time in Bowling Green. Finally, I would like to thank my advisor, Dr. Ajay Srivastava, who has accepted me and helped me grow during my time at WKU. To everyone above and those unnamed please know I appreciate everything you've done for me and you will always have my gratitude.

ACKNOWLEDGEMENTS

In addition to those listed in the dedication above, this thesis would not have been possible without the support of my thesis committee, Ogden College of Science and Engineering, and the WKU Graduate School. This thesis was supported by a Graduate School Research Grant and Department of Biology funds. Research in the Srivastava Lab is supported by KBRIN Area Grant funded from a parent NIH grant (#5P20RR016481-11) an RCAP-1 Grant (11-8032).

Special thanks to Dr. John Andersland for his patience and support with the microscopes at WKU. I would like to thank Mrs. Naomi Rowland for her technical support and assistance in the classroom. I would like to thank Christopher Fields for helping me begin my biology career at WKU by assisting and showing me a variety of experiments. Thanks to Hannah Watkins for assistance with the gel images. Thanks to my committee members for their support during their process. I would also like to acknowledge the support of all the Srivastava Lab members.

TABLE OF CONTENTS

1	Introduction	1
1.1	The Extracellular Matrix.....	1
1.2	Proteases.....	3
1.3	Cathepsin L	7
1.4	CP1 Encodes the Drosophila Cathepsin L Protease.....	13
1.5	Protease Inhibition.....	14
1.6	Wing Development.....	15
1.7	Drosophila melanogaster as a Model Organism	20
1.8	UAS-GAL4 and RNAi.....	21
1.9	Summary.....	24
2.	Materials and Methods	26
2.1	Drosophila Stocks and Cultures.....	26
2.2	Collagenase Assay.....	26
2.3	Immunohistochemistry.....	27
2.4	Cloning of Crammer into a PUASt Vector	28
3	Results	37
3.1	Over-expression of cp1 leads to an increase in collagenase activity	37
3.2	Overexpression of timp and cp1 mitigates effects of CP1 mediated BM degradation	39
3.3	Downregulating cp1 affects wingless signaling	42
3.4	Downregulating cp1 affects nubbin signaling.....	44
3.5	Downregulating cp1 does not affect vestigial signaling.....	46
3.6	Successful cloning and verification of the crammer cDNA into the vector pUASt 47	
4	Discussion and Future Directions	52
	Appendix	57
	References	59

CHARACTERIZING THE ROLE OF CP1 IN *DROSOPHILA MELANOGASTER*:
ITS EFFECTS ON BASEMENT MEMBRANE DEGRADATION AND SIGNALING

Dane Flinchum

May 2018

62 Pages

Directed by: Ajay Srivastava, Rodney King, Claire Rinehart

Department of Biology

Western Kentucky University

CP1 is a well-conserved cathepsin L-like protease essential for proper growth and development in *Drosophila melanogaster*. Previous research has demonstrated that CP1 has the ability to break down the extracellular matrix. Using the UAS-GAL4 system, immunohistochemistry, and antibody-staining, this research attempts to characterize the role of CP1 and its effects on basement membrane degradation and signaling. These effects include actions at the cellular level and on a known signaling pathway. The genes involved in this pathway are known to be required for proper development of the wing disc into the adult wing. We have demonstrated the collagenase activity of CP1 as well as a possible mechanism via TIMP. We have shown that *cp1* is part of the *wingless* signaling pathway and potentially acts as an upstream regulator on *wingless* and *nubbin*. Finally, we have successfully inserted the cDNA of a potential inhibitor of CP1, titled *crammer*, into the vector pUAST to create transgenic flies.

Understanding how CP1 affects *Drosophila* development through cellular and gene activity is important because cathepsins are highly conserved between flies, humans, and have been implicated in several diseases, including cancer. Discovering the mechanisms by which CP1 functions allows for discoveries to be made in connection with disease processes.

1 Introduction

The Srivastava laboratory is focused on understanding and characterizing extracellular matrix degradation and the factors that cause this activity. One goal of the laboratory is to understand what happens when extracellular matrix (ECM) breakdown occurs abnormally. Genes that have the potential to be an underlying cause of faulty ECM breakdown are the focus of studies in the laboratory. This research is related to tumor metastasis because cancers tend to co-opt or shut down regulatory mechanisms required for the degradation of ECM. In this study, we focused on a Cathepsin L cysteine protease, CP1, that is evolutionarily conserved in humans and model organisms like Mice, Zebrafish, and *C. elegans* (Table 1). The Cathepsin proteases have been implicated in several forms of cancer (CHAUHAN 1991; SUDHAN 2015) and CP1 has been demonstrated to be involved in cellular invasive behavior using a *Drosophila melanogaster* model (DONG 2015). In this study, data are provided that further our understanding of CP1 with respect to ECM degradation and cellular signaling.

1.1 The Extracellular Matrix

The extracellular matrix (ECM) is the non-cellular component of all tissues and organs and aids organs and tissues in strength, elasticity, and organization (Figure 1) (LIOTTA 1986; FRANTZ 2010). Although all ECMs are composed of the same basic components, it is a dynamic layer that undergoes constant remodeling. This remodeling can be enzymatic or non-enzymatic, and some changes to the molecular components involve post-translational modifications (LIOTTA 1986; FRANTZ 2010).

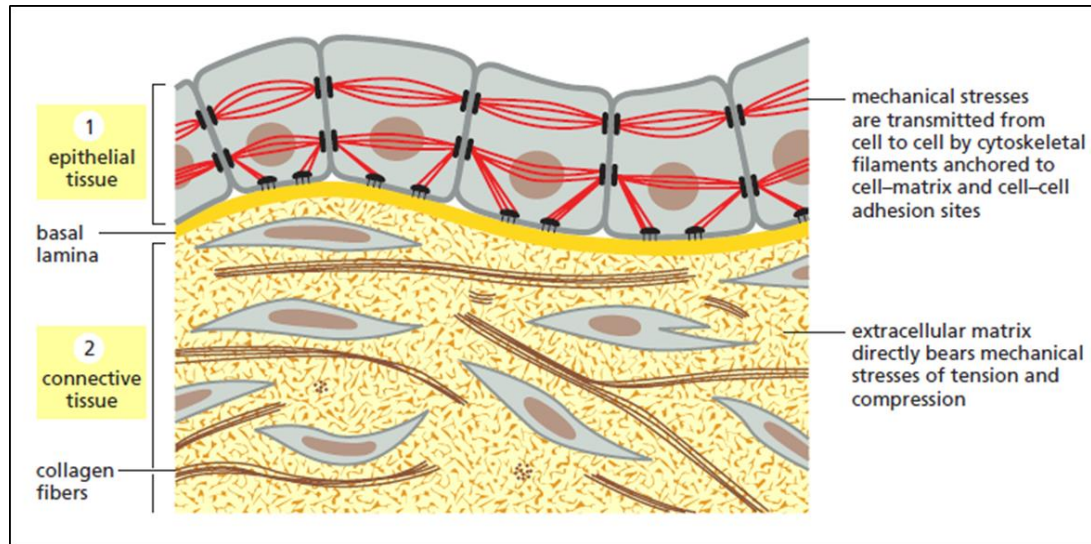


Figure 1: Layers of tissue, basement membrane, and the extracellular matrix.

The basement membrane separates tissues from the main connective tissue of the extracellular matrix (ALBERTS 2017).

The ECM is composed of proteoglycans and fibrous proteins such as collagen, laminins, elastins, and fibronectin (Figure 1). The physical and biochemical make-up of the ECM depends on the tissue it surrounds, and the specific composition arises during the development of the tissue (IGNOTZ 1986). Adhesion of cells to the ECM is mediated by specific receptors, such as integrins (IGNOTZ 1986). This adhesion is the underlying factor of cytoskeletal attachment to the ECM and is important for cellular migration through the ECM (FRANTZ 2010). Overall, the biological, protective, and organizational properties of the ECM vary strongly from tissue to tissue. The lungs require a different composition than bone, and bone requires a different composition than skin, and so on (FRANTZ 2010).

The basement membrane (BM) is a specialized layer of the ECM (Figure 1). It separates cells from connective tissue of the main ECM. The BM also provides support and modifies cellular behavior via signaling (LI 2003). The four major components of the BM are collagen IV, laminins, entacin, and perlecan (LEBLEU 2007). Type IV collagen and laminins individually assemble into super-structures. They provide the main structural stability of the basement membrane (LEBLEU 2007). Entacin and perlecan bridge the collagen and laminin structures.

1.2 Proteases

Proteases are enzymes that “cut” proteins by hydrolyzing peptide bonds and can be classified in several different ways. One way is by optimal pH, which includes acid, basic, and neutral proteases (RAWLINGS 2010). Another method is by catalytic residue. These include serine, cysteine, threonine, aspartic acid, glutamic acid, and matrix metalloproteinases. Finally, there is a MEROPS database that characterizes proteases by families and clans (RAWLINGS 2010). In this database, homologous proteins are grouped into families, which are further grouped into clans (RAWLINGS 2010). The classification focuses on distinguishing proteins by their specificity for cleaving at certain sites and how they interact with inhibitors (RAWLINGS 2010). The conservation of the cleavage site and its physiological relevance is important in classification as well.

Serine protease

Many proteases contain a catalytic triad, with the active site made of different amino acids depending on the type of protease. Serine proteases utilize a catalytic triad composed of serine, histidine, and aspartic acid (CAWSTON 2010).

This triad maintains proximity to each other due to the protein folding. Aspartic acid binds to the histidine, allowing histidine to pull protons from serine. This attraction enables serine to act as a nucleophile, “attacking” peptide bonds. Serine proteases are generally active at neutral pHs (CAWSTON 2010). *In vitro* experiments have demonstrated that serine proteases are upregulated during pro-inflammatory situations (SMITH 2010). Trypsin, chymotrypsin, and elastase are examples of serine proteases and are active during digestion, blood clotting, and ECM remodeling (SMITH 2010).

Threonine protease

Threonine proteases utilize a catalytic triad similar to serine proteases, except the serine is replaced with threonine (SCHAUER 2012). Research has demonstrated that threonine proteases participate in the degradation of ecdysteroid receptor isoforms. These isoforms control cell growth in *Drosophila melanogaster* and are known to be regulated by proteases (SCHAUER 2012).

Aspartic protease

Aspartic proteases utilize an acid-base mechanism for cleavage. One of the aspartates “attacks” a nearby water molecule, allowing the oxygen molecule to act as a nucleophile (DAVIES 1990). An intermediate molecule is formed before the –NH₂ group of the amino acid is removed. This protease requires an acidic pH, and thus does not generally act as an ECM remodeler because the ECM is usually around a pH of 7 (DAVIES 1990). Aspartic proteases help regulate blood

pressure by cleaving angiotensin and aid in digestion via the enzyme pepsin (DAVIES 1990).

Matrix Metalloproteinases

Matrix metalloproteinases are different from the previously mentioned proteases because they use a metal ion in their catalytic domain. This metal ion is usually zinc but can also be copper or another metal (VISSE 2003). The metal ion is held in place by three amino acids and activates a water molecule. This activation involves a similar process when compared to the catalytic triads mentioned previously. The proteinase domains contain a catalytic zinc, structural zinc, and three calcium ions (VISSE 2003). Three histidines are integral to maintaining catalytic zinc. An active zinc will bind to a peptide bond's carbonyl group. A water molecule is displaced from the catalytic triad and a reactive pocket accommodates the side chain of the target protein. This pocket accounts for specificity during binding and hydrolysis (VISSE 2003).

Drosophila have two metalloproteinases, MMP-1 and MMP-2 (PAGE-McCAW 2003). In contrast, humans have over 20 MMPs. The two *Drosophila* MMPs are more closely related to human metalloproteinases than they are each other (PAGE-McCAW 2003). MMP-1 has two splice forms, while MMP-2 contains no splice variants. Both MMPs are necessary for proper remodeling of the ECM, proper tubulogenesis, expansion of tubules, and proper degradation of the cuticle (PAGE-McCAW 2003) (SRIVASTAVA 2007). Research has demonstrated that *Drosophila* with MMP-1 mutations cannot remodel their cuticle and cannot

properly elongate their tubes, because they lack the ability to degrade the ECM (GLASHEEN 2010).

Tissue Inhibitors of Matrix Metalloproteinases

Proper development and remodeling of the ECM requires MMPs to act within a controlled environment. Tissue inhibitors of matrix metalloproteinases (TIMPs) are specific inhibitors of MMPs (HENRIET 1999; PAGE-MCCAW 2003). TIMPs function by occupying the active site of MMPs. There are four TIMP varieties in mammals but only one *Timp* gene in *Drosophila*. A deletion of *Timp* in *Drosophila* results in an inflated wing phenotype (PAGE-MCCAW 2003). When *Mmp2* was misexpressed, a glassy eye with flattened ommatidia phenotype occurred. When *Mmp2* and *Timp* were both coexpressed with an eye-specific *GMR-GAL4* driver, the phenotype was restored to nearly wild type levels via suppression of MMP. MMP misexpression phenotypes may be the result of inappropriate ECM degradation during development (SRIVASTAVA 2007).

Cysteine cathepsins

In humans, cysteine cathepsins are classified into Cathepsin B, C, F, H, L, K, O, S, V, W, and X. This classification is based on structure, substrate specificities, and catalytic mechanisms (RAWLINGS 2010). Although they were originally classified as intracellular proteins, studies have shown that classes B, K, and L assist in degrading the ECM and thus act extracellularly. Most cathepsins are part of normal cellular turnover, but some have become specialized for specific cells, such as Cathepsin K with osteoclasts (TURK 2012).

Cysteine cathepsins are almost all optimally active at an acidic pH due to their activity in lysosomes, and generally unstable at neutral pH. In a neutral pH, these cathepsins are often irreversibly inactivated. Cathepsins are involved in many normal physiological roles, including digestion, remodeling, and degradation (DUONG 2012).

Cysteine proteases use a catalytic triad, but with a thiol group (CAWSTON 2010). They have been implicated during ECM degradation and remodeling, cell growth, and development (DONG 2015). Cathepsins generally have three defined substrate binding sites. These sites are where substrate residues interact with main and side chain atoms of the protease (Figure 2) (TURK 2012). The active sites are composed of residues from four loops. Cathepsins tend to be redundant in their ability to cleave substrates, although their cleavage sites may not be at the same spot on the substrate (TURK 2012). Lysosomal cathepsins are synthesized as preproenzymes. The N-terminal signal peptide is removed as it passes through the endoplasmic reticulum. Then, the N-terminal propeptide is removed in the endosome (TURK 2012).

1.3 Cathepsin L

Cathepsin L is an important protease that is well conserved throughout several model organisms (CHAUHAN 1993; DENNEMÄRKER 2010; SUDHAN 2015). It aids in several physiological processes, particularly in controlled cellular and extracellular remodeling. Figure 3 shows the conservation of Cathepsin L through several model organisms, from humans to nematodes. Most of the differences

occur in the signal peptides, which are cleaved off before the protease becomes active. This illustrates the homology of cathepsin L

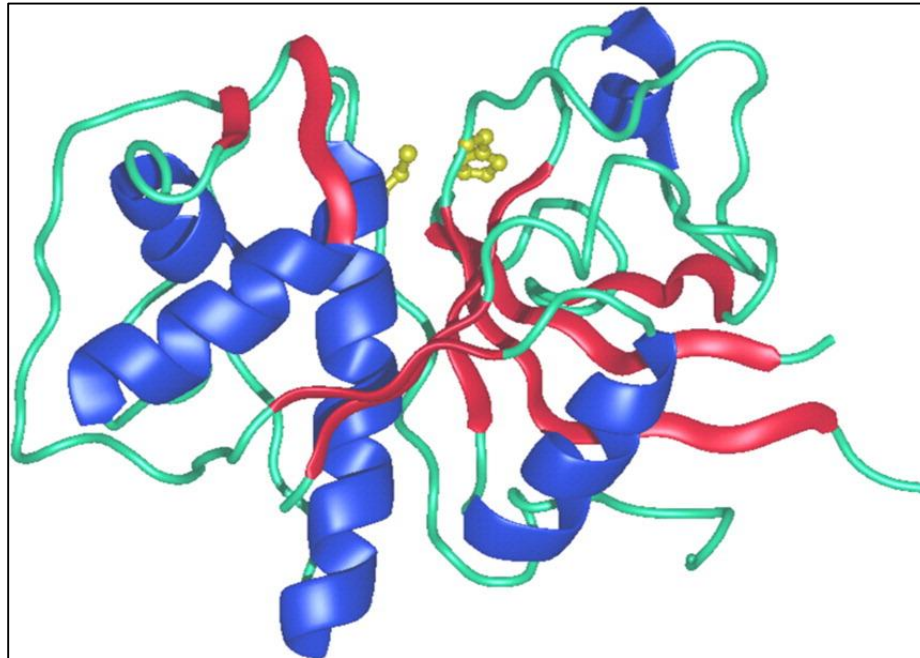


Figure 2: The mature form of human cysteine cathepsin endopeptidases. The green ribbon represents the fold of mature Cathepsin L while the blue and red represent secondary structures α -helices and β -sheets, respectively. The yellow ball and stick show the reactive cysteine (Cys25) and histidine (His163) (TURK 2012).

The crystal structure of the Cathepsin L protein has two domains, a left and right. The L domain has three α -helices while the R domain has a β -barrel with an active histidine at the top (TURK 2012). The center of these two domains has reactive site residues Cys25 and His163 (Figure 2). The active site in the center of these domains arises from four loops (TURK 2012). The L loops are

connected by a disulfide bond while the R loops are larger and form the core of the β -barrel. A target substrate is bound in the middle of these loops, while side chains alternate their binding with loops on either side (TURK 2012).

Cathepsin L is necessary for appropriate embryogenesis and development (Table 1) (BRITTON 2002). In *Caenorhabditis elegans*, the cathepsin L homologue is important for cell division and proliferation steps during embryogenesis. *C. elegans* only have one Cathepsin L and in Cathepsin L RNAi lines, slower cell division was seen and development eventually stopped with no observable morphogenesis (HASHMI 2002). In Zebrafish, the main isoform of cathepsin L is *ctsla*. Other isoforms in Zebrafish include *ctslb* and *ctslI*. The *ctsla* protein is found throughout embryogenesis and the adult stages and appears to be part of yolk processing during oogenesis and development (TINGAUD-SEQUEIRA 2007). As Table 1 shows, several different Cathepsin L's have been implicated in cancer growth. This association with cancer has been studied more extensively in human cell lines and mice. Cathepsin L's function has been shown to be conserved across the model organisms as depicted in Table 1 and Figure 3, and more opportunities for discoveries relating to tumor growth and metastasis potentially remain available in the less studied organisms.

Table 1: Examination of Cathepsin L in model organisms and their function and role in cancer. Several homologues have yet to be studied in depth

Organism	Protein (Gene)	Function	Relation to Cancer
<i>Homo sapiens</i>	Cathepsin L1 (<i>CTSL</i>)	Adaptive immune response, antigen processing, collagen catabolic process, proteolysis	Upregulated in colorectal, breast, pancreatic, lung, gastrointestinal, and melanoma cancers (SUDHAN 2015)
<i>Homo Sapiens</i>	Cathepsin L2 (<i>CTSL2</i>)	Antigen processing, autophagy, ECM disassembly, nerve development, proteolysis	Unknown
<i>Mus musculus</i>	Cathepsin L1 (<i>Ctsl</i>)	Autophagy, cell communication, protein processing, proteolysis	Ctsl mRNA and cathepsin activity upregulated in a pancreatic neuroendocrine tumorigenesis model (BRINDLE 2015); Mice with ctsl deficiency had enhanced tumor expression (DENNEMÄRKER 2010)
<i>Rattus norvegicus</i>	Cathepsin L1 (<i>Ctsl</i>)	Adaptive immune response, autophagy, cell communication, protein processing, proteolysis	Unknown
<i>Danio rerio</i>	Cathepsin La (<i>ctsla</i>)	Proteolysis in cellular protein catabolic process	Unknown
<i>Danio rerio</i>	Cathepsin Lb (<i>ctslb</i>)	Proteolysis in cellular protein catabolic process	Unknown
<i>Danio rerio</i>	Cathepsin L, like (<i>ctsl</i>)	Unknown	Unknown
<i>Drosophila melanogaster</i>	Cathepsin L (<i>CP1</i>)	Digestion, development, proteolysis, catabolism, cellular invasion	Breakdown of BM by tumors is necessary for invasion and this is prevented by TIMP (DONG, SRIVASTAVA UNPUBLISHED)
<i>Caenorhabditis elegans</i>	Cathepsin L (<i>CPL-1</i>)	Proteolysis involved in cellular protein catabolic process, development, embryogenesis	Unknown

Cathepsin L is necessary for proper growth and development, but it can be utilized for negative consequences by cancerous cells. Cathepsin L is a known BM degrader in vitro and can potentially facilitate the spread of tumorigenic cells to the bloodstream or other areas of an organism (SUDHAN 2016). High levels of Cathepsin L have been observed in human breast cancer cells, and these patients were at a significantly higher risk of relapse, metastasis, and death (SUDHAN 2016). When endothelial cells encounter Cathepsin L during tumor angiogenesis, they increase in their ability to migrate and invade (SUDHAN 2016).

Human L1	1	MNPTLILAAFLCLGIASATLTFDHSLE---AQWTKWKAMHNRLYGMNEEG-WRRRAVWEKNMKMIELHNQYREGKHSFTMA	76
Human L3	1	-----MKMIEQHNQYREGKHSFTMA	21
Rat	1	MTPLLLLAVLCLGTALATPKFDQTFN---AQNHQWKS THRRLYGTNEEE-WRRRAVWEKNMRMIQLHNQGEYSNGKHGFTME	76
Mouse	1	MNLLLLLAVLCLGTALATPKFDQTFN---AENHQWKS THRRLYGTNEEE-WRRRAIWEKNMRMIQLHNQGEYSNGQHGF SME	76
ZebrafishA	1	MRVFLAAFTLCLSAVFAAPTLDQQLN---DHNDQWKKWHSKKYHATEEG-WRRRIWEKNLKKIEMHNLEHSMGIHTYRLG	76
ZebrafishB	1	M-MFALLVTLCLISAVFAASSIDIQLD---DHNWSWKSQHGKSYHEDVEV-GRRMIWEENLRKIEQHNF EYSYGNHTFKMG	75
<i>C. elegans</i>	1	MNRFILLLAVAVAVNSAKLSRQIEsaIEKNDYKEDFDKEYSESEEQ-TYMEAFVKNMIHIEHNHRDHRLGRKTFEMG	79
<i>Drosophila</i>	1	MRTAVLLPLLALAVAVAVSADVVM---EENHTFKLEHRKNYQDETEERFLRKIFNENKHKIAKHNRQFAEGKVSFKLA	77
Human L1	77	MNAFGDMTSEEFQVMNGFQNRKPR KGVQFQEPLFYEAPRSVDWREKGYVTPVKVQCGSCWAFSATGALEGGMFR	153
Human L3	22	MNAFGEMTSEEFQVVNGFQNRKPR KGVQLQEPLLDHIRKSVDWREKGYVTPVKDQCNWGSVRT-----DVR	88
Rat	77	MNAFGDMTNEEFQIVNGYRHKQHK KGRLFQEPLMLQIPKTVDWREKGCVTPVKVQCGSCWAFSASGCGLEGGMFL	153
Mouse	77	MNAFGDMTNEEFQVVNGYRHKQHK KGRLFQEPLMLKIPKSVDWREKGCVTPVKVQCGSCWAFSASGCGLEGGMFL	153
ZebrafishA	77	MNHFGDMTHEEFQVMNGFKKDKDR [2]RGS LFMENFIEV PNKLDWREKGYVTPVKDQCGECSCWAFSTTGALEGGMFR	155
ZebrafishB	76	MNQFGDMTNEEFQAMNGYKHPNR [2]QGFLMEPSFFAAPQQVDWRQRFVTPVKDQKCGSCWFSSTGALEGG LFR	154
<i>C. elegans</i>	80	LNHIADLPFSYQRK-LNGYRRLFGD [4]N SSSFLAPFNVQVPDEVDWRDTHLVTDVKNQGMCGSCWAFSATGALEGGHAR	159
<i>Drosophila</i>	78	VNKYADLLHHEFRQLMNGFNYLHK [9]KGVTFISP AVTLPKSVDWRTKGAVTAVKQCGHSCWAFSSTGALEGGHFR	163
Human L1	154	KTGRLISLSEQNL VDCSGPQGNEGCNGGLMDYAFQYVQDNGGLDSEESYPYEATEE-SCKYNPKYSVANDTGFVDI	228
Human L3	89	KTEKLVLSVQTW [35]FHMKSSGDWVKVQGHRSAGESLLASGESQSQSPEVAQYSGKHQVQCHLIEEALQMLSGGDH	199
Rat	154	KTGKLVLSLSEQNL VDCSHDQGNQGCNGLMDFAFQYIKENGLDSEESYPYEAKDG-SCKYRAEYAVANDTGFVDI	228
Mouse	154	KTGKLVLSLSEQNL VDCSHAQGNQGCNGLMDFAFQYIKENGLDSEESYPYEAKDG-SCKYRAEFVAVANDTGFVDI	228
ZebrafishA	156	KTGKLVLSLSEQNL VDCSRPEGNEGCGNGLMDQAFQYVVDQNGLDSEESYPYLGTDQPCHFDPKNSAANDTGFVDI	231
ZebrafishB	155	KTGKLVLSLSEQNL VDCSRPQGNQGCNGLMDQAFQYVVDQNGLDSEESYPYLRDDIPCRYPDRFNVAKITGFVDI	230
<i>C. elegans</i>	160	KLGLVLSLSEQNL VDCSTKYGNHGCNGLMDQAFYIRDNHGVDTEESYPYKGRDM-KCHFNNKTVGADDKGYVDI	234
<i>Drosophila</i>	164	KSGVLVLSLSEQNL VDCSTKYGNNGCNGLMDNAFRYIKDNGGIDTEKSYPYEAIDD-SCHFNNKTVGATDRGFVDI	238
Human L1	229	PK-Q-EKALMKAVATVGPI SVAIDAGHESFLFYKEGIYFEPDCSS EDDMDHGVLVVGYGFESTEDNKNYWLKNSWGEW	306
Human L3	200	DEDKwPHDMRNHLAGEAQV-----	218
Rat	229	PQ-Q-EKALMKAVATVGPI SVAMDASHPLQFYSSGIYYEPCSSKLDHGVLVVGYGEGTDSNKKYWLKNSWGWKEW	306
Mouse	229	PQ-Q-EKALMKAVATVGPI SVAMDASHPLQFYSSGIYYEPCSSKLDHGVLLVGYGEGTDSNKNKYWLKNSWGSWEW	306
ZebrafishA	232	PSGK-ERALMKAIAAVGPI SVAIDAGHESFQFYQSGIYYEKECSSELDHGVLVAVGYGFEGEDVDGKKYVIVKNSWSEW	310
ZebrafishB	231	PRGN-ELALMNAVAAGPI SVAIDASHQLQFYQSGIYYERACSSRLDHAVLVVGYGQGADVAGNRYVIVKNSWSDKW	309
<i>C. elegans</i>	235	PEGD-EEQLKIAVATQGPISIAIDAGHRSFQLYKKGVIYDEECSSELDHGVLLVGYG---TDPEHGDYVIVKNSWAGW	310
<i>Drosophila</i>	239	PQGD-EKKMAEAVATVGPI SVAIDASHESFQFYSEGVIYNEPQCDAQNLDHGVLVVGF---TDESGEDYWLKNSWGTW	314
Human L1	307	GMGGYVKMAKDRRNHCGLASASYPV-	333
Human L3		-----	
Rat	307	GMDGYIKIAKDRNHCGLATAASYPIVn	334
Mouse	307	GMEGYIKIAKDRNHCGLATAASYPVn	334
ZebrafishA	311	GDKGYIYMAKDRNHCGLATAASYPLV-	337
ZebrafishB	310	GDKGYIYMAKDRNHCGLATAASYPLM-	336
<i>C. elegans</i>	311	GEKGYIRIARNRNHCGLATAASYPLV-	337
<i>Drosophila</i>	315	GDKGFIKMLRNKENQCGIASASYPLV-	341

Figure 3: Cathepsin L Homology in Model Organisms. The red color indicates amino acid homology while the gray indicates differences. The gray at the beginning are signal peptides that are cleaved off before activation. All the Cathepsin L's are similar in size, from 333-341 amino acids.

1.4 CP1 Encodes the *Drosophila* Cathepsin L Protease

The *Drosophila* version of Cathepsin L is titled Cathepsin L cysteine protease or CP1 (TRYSELIUS 1997). The protein is 341 amino acids long and contains two well-conserved domains: the inhibitor I29 domain and endopeptidase domain commonly seen in Cathepsin L proteins (Figure 4). The inhibitor domain prevents substrates from approaching the active sites of the cathepsin. Cleavage of this domain can activate the protein from its zymogen state (TRYSELIUS 1997).

Matsumoto et al isolated the *cp1* gene and found that it was mostly expressed in the midgut and salivary gland of *Drosophila* (MATSUMOTO 1995). Tryselius and Hultmark isolated cDNA clones encoding the full-length CP1 sequence in a *Drosophila* hemocytic mbn-2 cell line (TRYSELIUS 1997). They hypothesized that CP1 performed an immune function by participating in the degradation of internalized material in phagocytic cells. Recently, an expression screen identified CP1 as a regulator of *Drosophila* sensory field innervation. A class of *Drosophila* neurons can elaborate two distinct dendritic trees through complete pruning and regeneration (LYONS 2014).



Figure 4: The inhibitor I29 Domain and Peptidase C1 domain of *Drosophila*'s cathepsin L cysteine protease (CP1).

1.5 Protease Inhibition

Inhibition of cathepsins is usually performed by cystatins and stefins (type 1 cystatins), which bind reversibly (TURK 2012). These inhibitors have a five-turn α -helix and five-stranded antiparallel β -pleated sheet. The N-terminal and two hairpin loops are required for interaction with the target cathepsins (TURK 2012). Cystatin M/E strongly inhibits human cathepsin L in skin and Stefin B inhibits cathepsin L in cytosol and cell nuclei (CHENG 2006) (ČERU 2010).

Cystatins are often emergency inhibitors, reacting to escaped proteases or proteases of invading pathogens (TURK 2012). In *Drosophila*, a single gene has been identified as a cystatin (DELBRIDGE 1990). A proteomics study showed that several cystatin-like proteins are expressed in the hemolymph of *Drosophila* larvae (VIERSTRAETE 2003). Cystatins appear to function as non-specific inhibitors of the cathepsin family, not just Cathepsin L (DESHAPRIYA 2007).

In addition to being inhibited by cystatins and stefins, another protein has been shown to inhibit CP1 *in vitro* (NGA 2014). This protein, Crammer, is approximately 79 amino acids long and its inhibition depends on the pH level (TSENG 2012). Crammer contains four α -helices and the C-terminal region blocks the cathepsin active site. Crammer is unrelated to cystatins and has sequence similarities to the proregions of CP1 (NGA 2014).

Deshapriya et al examined the cysteine inhibitor *Drosophila* CTLA-2-like protein (D/CTLA-2), the gene product of *crammer*. Recombinant D/CTLA-2 expressed in *E. coli* strongly inhibited *Bombyx* cysteine protease, as well as human Cathepsin L and H. The recombinant D/CTLA-2 also acted as a potent

inhibitor of CP1, indicating that the cathepsin is a target of this enzyme. D/CTLA-2 appears to act as a selective inhibitor of CP1 (DESHAPRIYA 2007).

When recombinant crammer was incubated with purified CP1, only the monomeric form of crammer, not the dimer, exhibited inhibitory activity towards CP1. Before the proregion of CP1 is cleaved, the inhibitor domain with two C-terminal residues blocks the active site. The crammer protein blocks the active site of the cathepsin in a similar way topologically (DESHAPRIYA 2007). However, the sequences of the proregions are different and crammer's chain is longer and free of cysteine.

1.6 Wing Development

The *Drosophila* wing develops from a wing imaginal disc, an epithelial sac containing 50,000-75,000 cells during late third instar stage. The wing imaginal disc contains the primordia for the adult wing, including the notum, hinge, blade, and margin. The development, polarity, and patterning of the adult wing structures is regulated by several interactive genes. One of the most crucial and well-studied of these regulatory genes is *wingless (wg)* (BEJSOVEC 2013).

Because *wg* is a *wnt-1* homologue, this has allowed the role of Wnt proteins during development to be studied extensively (SWARUP 2012). The Wnt signaling pathway is an evolutionarily conserved cell signaling pathway that regulates development throughout embryogenesis and adult homeostasis. The Wnt pathway regulates cell proliferation, cell polarity, and specification of cell fate. Sequence similarity to the first Wnt protein discovered (Wnt-1) determines

members of the Wnt family. There are 19 Wnt proteins in vertebrates, and *Drosophila* have seven homologues.

The Effects of wingless on Drosophila Development

Secreted signaling molecules such as *wg* help coordinate the growth and patterning of groups of cells in *Drosophila*. The expression of *wg* in certain groups of cells allows it to function as an organizing center to direct the proper growth pattern of surrounding tissue. Cells determine their position based on how far away they are from the signaling center. This information is based on a concentration gradient of the *wg* signal (NEUMANN 1996). In the wing disc, *wg* signaling is necessary for proper development of the dorsal-ventral (DV) boundary. Localized expression of *wg* at the DV boundary can act at long-ranges to activate other genes and control growth of the wing (NEUMANN 1996).

Wg signaling is necessary not only for *Drosophila* wing development, but other structures as well. Wu *et al* demonstrated that *wg* is specifically required for heart development (WU 1995). When *wg* was knocked out just after gastrulation, heart precursors were lost. *Wg* also plays a role in segmentation and neurogenesis. In a developing *Drosophila* epidermis, *wg* is expressed in a single row of cells in each segment. *Wg* signaling promotes specification of the intrasegmental pattern (HAYS 1997).

The *Drosophila* central nervous system develops from neural stem cells called neuroblasts. Neuroblasts develop from the ectoderm in a fixed pattern, and their position within this pattern determines their fate and function. *Wg* is

required for neuroblasts to develop in different anteroposterior positions to determine different fates. *Wg* and *gooseberry* act together as segment polarity genes to determine cell fates (SKEATH 1999).

The Effects of wingless on Drosophila Wing Hinge Development

During the third instar larval stage, *wg* is expressed in two ring-like domains in the hinge region. The expression occurs along the dorsal/ventral compartment and divides the wing blade (Figure 5). The inner-ring area frames the wing blade and develops into the hinge while the dorsal ventral boundary forms the wing margin. In *spade* mutants, *wg* expression is removed from the inner ring. *Spade* mutants result in the hinge region being deleted and the wing pouch appears to be joined to the proximal cells nearby. There is a general underproliferation of cells suggesting that *wg* promotes local cell growth (NEUMANN 1996).

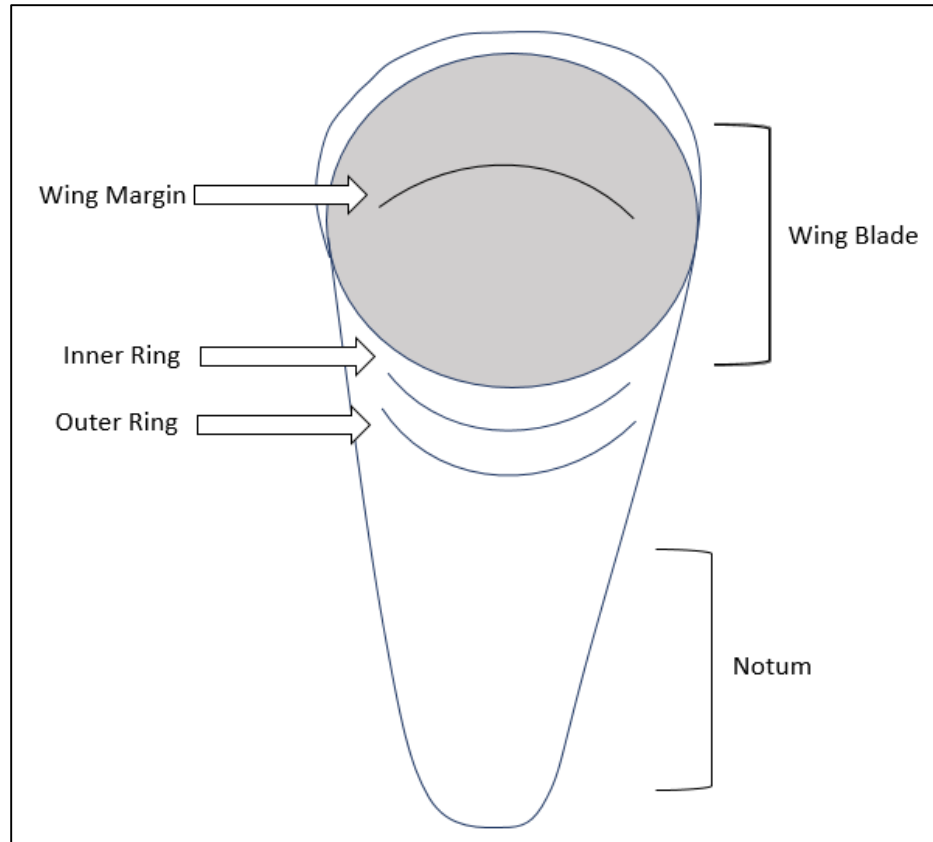


Figure 5: Wingless Expression in Wing Imaginal Disc. Expression can be seen in the inner and outer rings of the wing hinge, as well as in the wing pouch at the dorsal-ventral boundary.

The genes *wg*, *nubbin* (*nub*), and *rotund* (*rn*) are required for proper development of the wing hinge (DEL ÁLAMO RODRÍGUEZ 2002). The *rotund* gene codes for a member of a zinc-finger transcription factor family, while the *nubbin* gene encodes a member of the POU family of transcription factors (DANTOFT 2013). POU homeobox transcription factors are sequence-specific DNA binding proteins that regulate transcription (DANTOFT 2013). This family can bind as homodimers or heterodimers (with other members of the family) to DNA. A *rn* mutation results in deletion of the wing hinge and no *wg* expression in the inner

ring. A *nub* mutation can have various effects. Strong mutations result in vestigial wings, while weaker mutations can result in wing hinge deletion and no expression of *wg* in the inner ring (DEL ÁLAMO RODRÍGUEZ 2002). When lower levels of *nub* are present within wing discs, *rn* experiences significant down-regulation. Transcription of *rn* is thought to be regulated in some manner by the amount of *nub* (MATTA ET AL 2011).

Vestigial (*vg*) encodes a nuclear protein that is suggested to mediate transcriptional activation (DEL ÁLAMO RODRÍGUEZ 2002). Expression of *vg* in the wing is regulated by the boundary enhancer and the quadrant enhancer (DEL ÁLAMO RODRÍGUEZ 2002). In mature wing discs, *vg*, *rn*, and *nub* are expressed in three concentric domains. When a null allele of *vg* was used, there was no observable expression of *wg*, *rn*, and *nub* in the wing pouch (Figure 6). This result was observed in earlier wing disc stages as well, suggesting that the *vg* protein is required for the expression of *wg*, *rn*, and *nb* in the wing pouch (DEL ÁLAMO RODRÍGUEZ 2002).

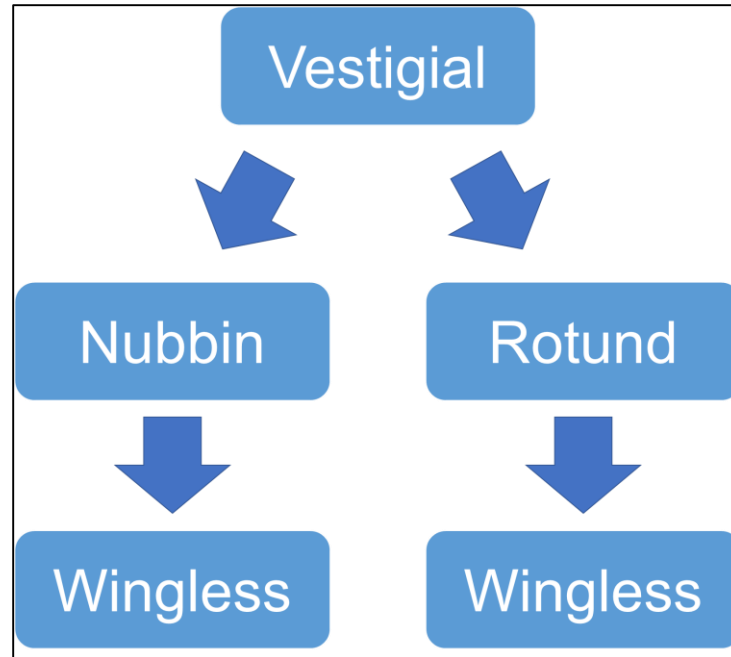


Figure 6: Schematic showing four genes within the *wg* signaling pathway with *vg* as the upstream regulator necessary for *wg*, *nub*, and *rn* expression during hinge development.

1.7 *Drosophila melanogaster* as a Model Organism

We utilized *Drosophila melanogaster* in this study because they are small, inexpensive, easy to care for, have short distinct life stages, and have well-known and understood genetics. *Drosophila* are a superb genetic model for studying disease because they have approximately 75% of the disease-causing genes that humans possess (REITER 2001). These qualities and the UAS-GAL4 system allow for controlled expression of desired genes with the proper mating patterns (BRAND 1993).

The *Drosophila* life cycle begins with fertilization of the embryo (Figure 7). After fertilization, *Drosophila* embryos develop into first instar larva in about 1

day. After 1 more day, they develop into 2nd instar larva and about a day after that they become 3rd instar larva. At this stage, the larvae are motile for about two days. They spend this time eating, storing energy, and preparing to pupate. Emergence from the pupa occurs about 4 days after the pre-pupa forms.

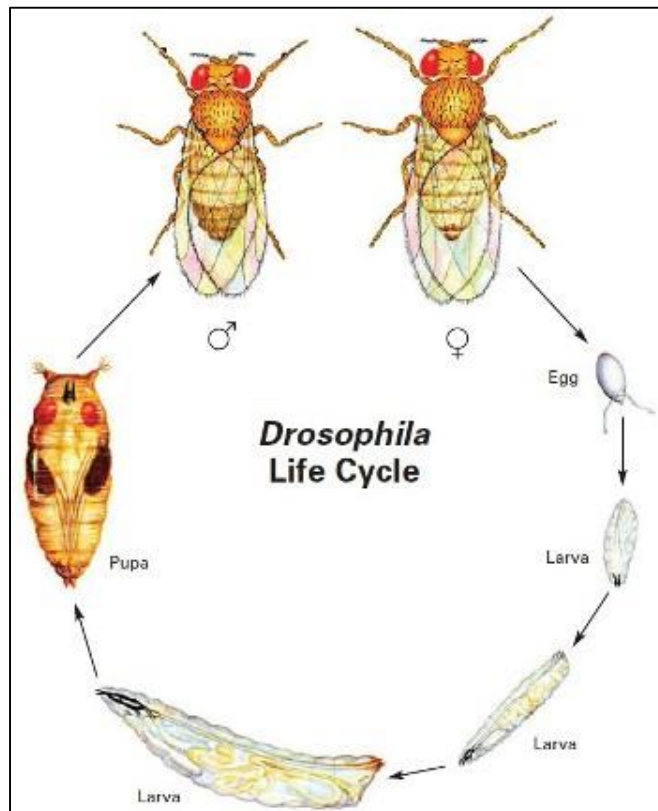


Figure 7: The life cycle of *Drosophila melanogaster*. Offspring go from egg to adult in roughly 10 days. Wandering third instar larva appear about 7 days after fertilization. (Image Source: Raymond Flagg, Carolina Biological Supply Company)

1.8 UAS-GAL4 and RNAi

Andrea Brand and Norbert Perrimon introduced the UAS/GAL4 system in 1993 as a method of targeted gene expression in *Drosophila* that allows for

selective activation of cloned genes (BRAND 1993). One parental line has the regulator, GAL4, which acts as a driver of gene expression. The other parental line has a responder gene, which needs the GAL4 protein to bind to the Upstream Activation Sequence (UAS) to initiate transcription. Figure 8 shows that when offsprings only have either GAL4 or UAS, no expression of the targeted gene occurs. However, when offsprings have both elements, expression of the targeted gene occurs in a pattern that reflects the GAL4 driver (DUFFY 2002).

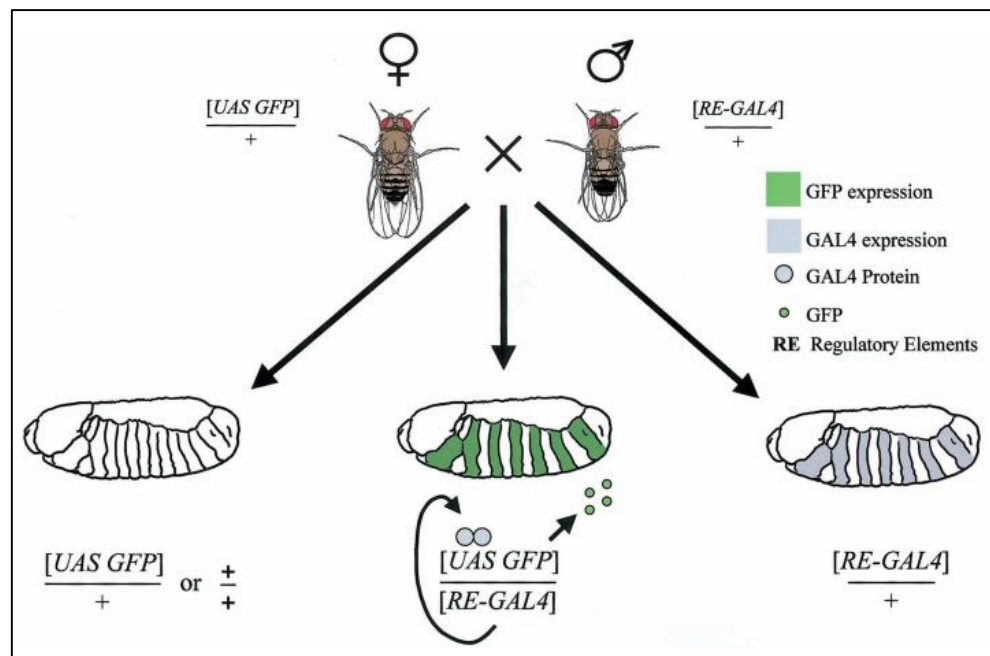


Figure 8: The Mechanism of UAS/GAL4 Expression from *Drosophila* adults to larva. Offspring that have both the UAS insert and the GAL4 insert can express the targeted gene. Larva without both of these characteristics are unable to express the targeted gene (DUFFY 2002).

RNA-mediated interference (RNAi) technology is used in conjunction with the UAS/GAL4 system to analyze loss-of-function phenotypes (Figure 9). An RNAi site can be attached to the gene of interest to downregulate expression. When the RNAi site is attached to the UAS and gene of interest, GAL4 protein binds to the UAS and double stranded RNA is generated when a hairpin is formed. Dicer recognizes and approaches the double stranded RNA hairpin and cleaves it into small interfering RNAs (siRNAs). These small pieces are separated into single strands and integrated into the RISC complex. This complex will base-pair with the targeted mRNA and cleave it, preventing translation from occurring (DUFFY 2002).

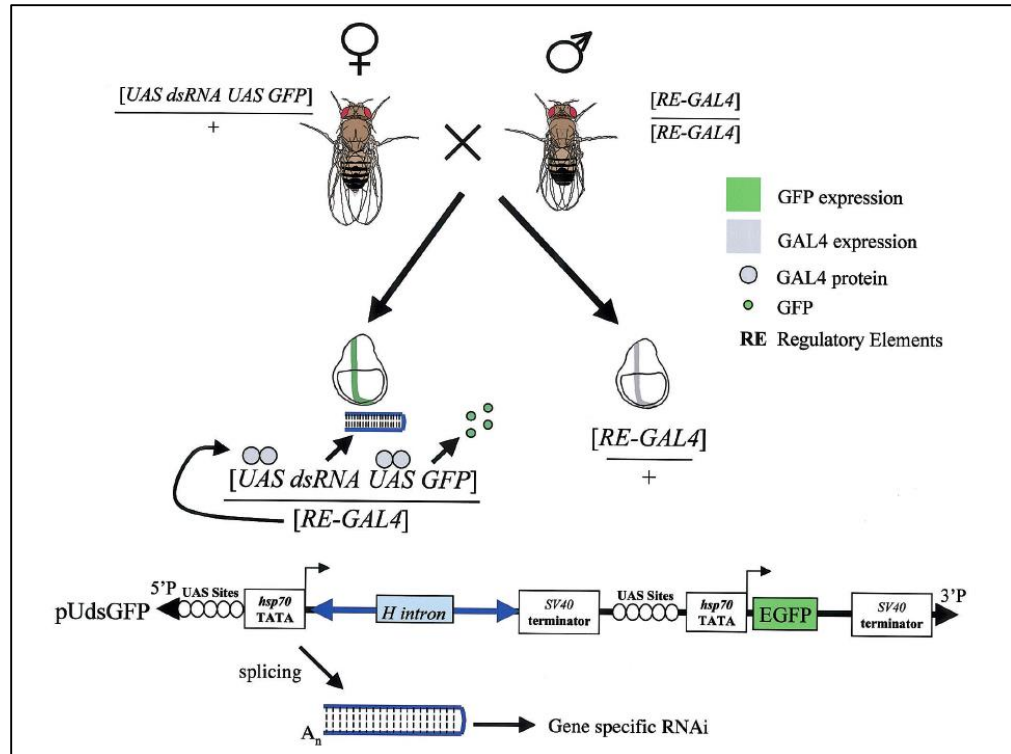


Figure 9: Mechanism of RNA-mediated interference. When offsprings have the UAS dsRNA and RE-GAL4, double stranded RNA is generated when a hairpin is formed. This is eventually assimilated into the RISC complex and will base-pair with targeted mRNA to cleave it.

1.9 Summary

Previous research in the Srivastava lab demonstrated that CP1 is expressed in dorsal air sac primordium (ASP) and overexpression of CP1 increases collagenase activity. Our data supports that conclusion with additional evidence from a larger number of wing discs. We examined the potential mechanisms of CP1 activity through the use of MMPs. By overexpressing both *CP1* and *timp*, we aimed to discover whether TIMP activity would inhibit CP1 and restore collagenase levels to wild type baselines. We also wanted to discover

whether *CP1* was part of the *wg* signaling pathway in the wing disc by knocking out *CP1* with an RNAi line and monitoring the expression of *wg*, *nub*, *m*, and *vg* using antibody staining. Finally, we wanted to examine the effects of *crammer* *in vivo* in *Drosophila*. This was performed by cloning the *crammer* sequence into a pUAST plasmid to create transgenic flies.

2. Materials and Methods

2.1 *Drosophila* Stocks and Cultures

Fly crosses were set up at 25°C, unless otherwise stated, in *Drosophila* media using standard conditions. *Ptc-gal4,UAS-srcRFP/CyO* was used to overexpress *CP1* in the wing for collagenase assays and antibody stainings.

Table 2: Stocks Used in This Study

Stock	Purpose
<i>UAS-CP1-3XHA</i>	Used to overexpress <i>cp1</i>
<i>UAS-CP1-3XHA x Ptc-gal4,UAS-srcRFP/CyO</i>	Used to overexpress <i>cp1</i> in wing disc
<i>W (UAS-TIMP, w+)/FM7</i>	Used to overexpress <i>timp</i>
<i>W (UAS-TIMP, w+)/FM7; Ptc-gal4,UAS-srcRFP; UAS-CP1-3XHA</i>	Used to overexpress both <i>timp</i> and <i>cp1</i> in wing disc
<i>Ptc-gal4,UAS-srcRFP/CyO</i>	Used to overexpress <i>cp1</i> along posterior/anterior boundary in wing disc
<i>UAS-CP1-RNAi/CyO; UAS-DCR2/TM₆Tb</i>	Used to knock-out <i>cp1</i> expression
<i>Sco/CyO; Sb/ TM₆Tb</i>	Double Balancer line

2.2 Collagenase Assay

Third instar larvae were dissected in cold 1X PBS and incubated in a staining solution (100ug/mL fluorescein conjugated DQ Gelatin in 1X PBS) for 90 minutes at room temperature. The larvae were fixed in a 4% paraformaldehyde fixative solution for 30 minutes at room temperature and washed in 1X PBS. The wing discs were dissected out and mounted in Vectashield Mounting Medium

(Vector Laboratories). A Carl Zeiss Axioplan 2 Imaging Fluorescent Microscope was used to image the samples.

2.3 Immunohistochemistry

The primary antibody for *wingless* was used at 1:50 dilution, for *vestigial* at 1:100 dilution, and for *nubbin* at 1:100 dilution. All secondary mouse antibodies were used at 1:500 dilutions (Table 3). Anti-mouse 488 was used for *wingless* and *nubbin* stainings, while anti-rabbit 488 was used for *vestigial* stainings (Table 3). Approximately 20 third instar larvae were dissected in cold 1X PBS. After the dissection was finished, the PBS was removed and 1mL of fixative was added and the larvae were rocked for 10 minutes. The fixative was removed and the larvae washed 2X with PBTA for 20 minutes each. The PBTA was removed and 760µL of fresh PBTA and 40µL of Goat Serum was added, along with the appropriate primary antibody dilution. This mixture was rocked overnight on a Nutating Mixer (Labnet International). The next morning, the mixture was removed and the larvae were rinsed with fresh 1X PBTA. Next, the larvae were washed 4X with PBTA for 15 minutes each. A fresh 760µL aliquot of PBTA was added along with the secondary mouse antibody dilution at 1:500. This was rocked for 90 minutes at room temperature. Afterwards, the larvae were washed 4X with PBTA for 15 minutes each. After the final wash, the wing discs were removed from the larvae, mounted in Vectashield with a coverslip, and imaged using a Carl Zeiss Axioplan 2 Imaging Fluorescent Microscope.

Table 3: Antibodies Used in this Study

Gene	Primary Anitbody	Secondary Antibody
<i>Wingless</i>	<i>Anti-wg (1:50)</i>	<i>Anti-mouse 488 (1:500)</i>
<i>Nubbin</i>	<i>Anti-nub (1:100)</i>	<i>Anti-mouse 488 (1:500)</i>
<i>Vestigial</i>	<i>Anti-vg (1:100)</i>	<i>Anti-rabbit 488 (1:500)</i>

2.4 Cloning of Crammer into a PUASt Vector

A pUCIDT-AMP : CramEcoXho plasmid with the *crammer* cDNA was ordered from Integrated DNA Technologies according to the published *crammer* cDNA sequence and the pUASt samples were obtained from the Srivastava lab stocks (Figures 10 and 11). The *crammer* sequence was digested out of the plasmid and inserted into the pUASt. This insertion was performed by ligation (details in the following section), DH5 α transformation, and miniprep. The insertion was confirmed by digesting the final pUASt with the insert and sequencing with a Thermo-Fisher 3130 Sequencer.

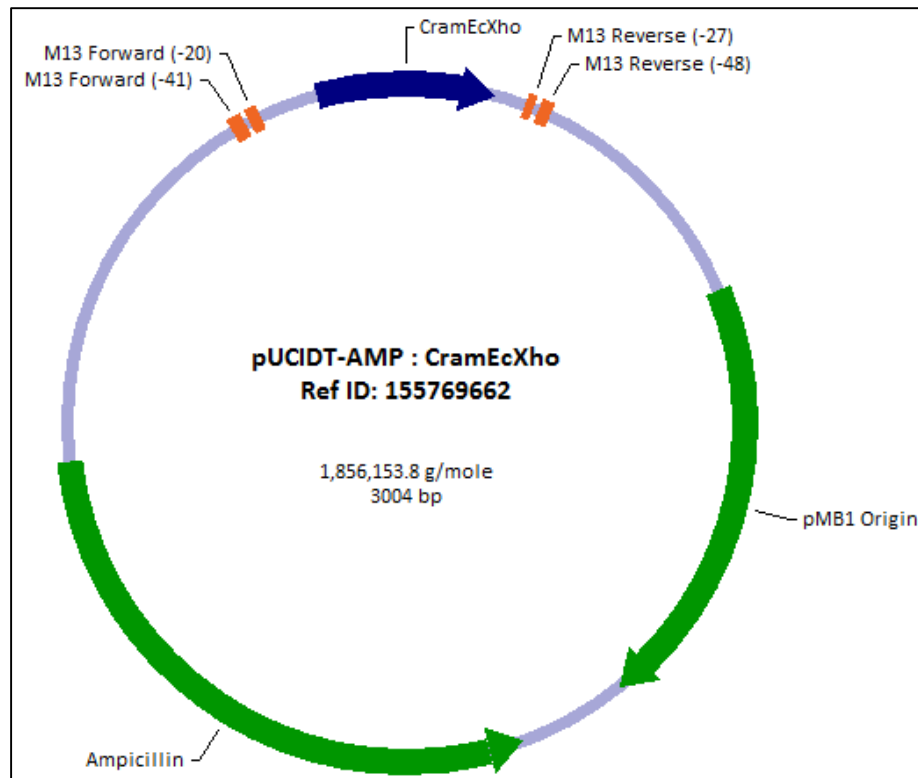


Figure 10: Map of pUCIDT-AMP: CramEcoXho Plasmid. The crammer sequence in blue was excised with EcoR1 and Xho1.

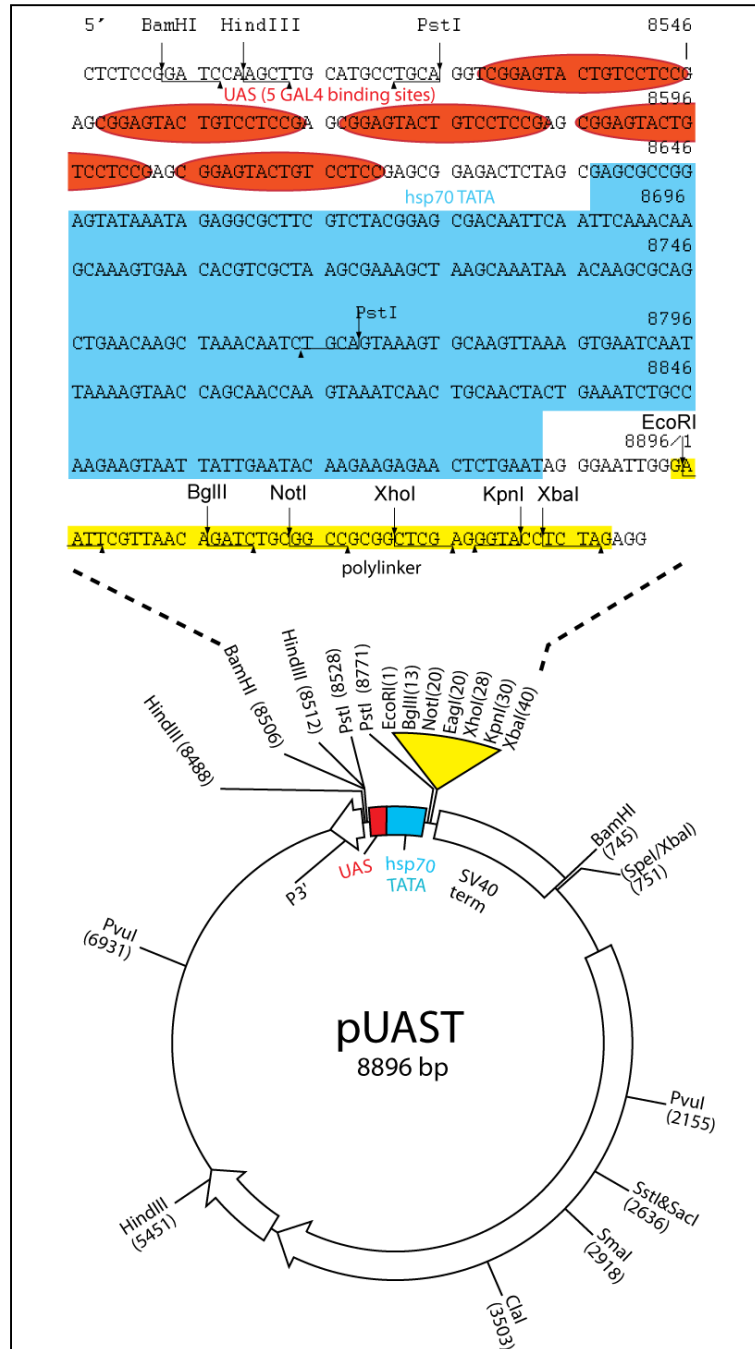


Figure 11: Map of pUAST. EcoR1 and Xho1 were used to digest open the plasmid to insert the crammer sequence (BRAND 1993).

Digestion

The pUCIDT-AMP : CramEcoXho plasmid and pUAST plasmid were digested with Buffer H , EcoR1 and Xho1 for 2.5 hours at 37° C (Table 4). Buffer H (Lot #A1501A) was purchased from Invitrogen, while EcoR1 (Lot #00532622), and Xho1 (Lot #00553975), were purchased from Thermo Scientific. 10X Loading Dye was added after the digestion was complete. The samples were run on a 1% TAE gel for 60 minutes at 100V. Once the gel was run and visualized using ethidium bromide and UV light, the samples were cut out of the gel and weighed. The *crammer* cDNA is 240bp and the excised gel fragment was between the 200bp and 300bp rungs of the 1Kb+ DNA Ladder (LabTech/Invitrogen).

Table 4: Digestion Reagents

Reagent	Amount
Plasmid DNA	20 μ L
EcoR1	2.5 μ L (10U/ μ L)
Xho1	2.5 μ L (10U/ μ L)
Buffer H	2.7 μ L (10x)
Total	27.7μL

Gel Extraction

The DNA gel extraction was performed with the QIAEX II Gel Extraction Kit (Catalogue #20021, Qiagen Inc.). The excised gel slice between the 200bp and 300bp rungs of the ladder containing *crammer* cDNA received 3 volumes Buffer QXI and the pUAST DNA received 3 volumes Buffer QXI and 3 volumes water (due to a higher concentration of DNA). Buffer QIAEX II was vortexed for

30s and 30 μ L was added to both samples. The gel slices were incubated at 50°C in a heating block for 10 minutes while being vortexed every 2 minutes. After the incubation, the samples were centrifuged in a conventional table-top microcentrifuge for 30 seconds at 17,900xg. After centrifugation, the supernatant was removed and the pellets washed with 500 μ L Buffer QXI. The pellets were resuspended by vortexing and flicking the tube. The samples were centrifuged again for 30s at 17,900xg and the supernatant removed. The pellets were washed twice with Buffer PE and resuspended by vortexing. The supernatant was removed and the pellets were vacuum-dried until they turned white. Twenty microliters of water were added and the pellet was resuspended. The *crammer* sample was incubated at room temperature for 5 minutes and the pUAST was incubated at 50° C for 5 minutes. After the incubations were complete, the samples were centrifuged for 30s and the supernatant was stored. A Nanodrop was used to determine the concentration and purity of the extracted DNA.

Ligation

The gel extracted *crammer* cDNA was ligated into the pUAST using T4 DNA ligase (Purchased from New England Biolabs, Catalogue #M0202S). Three different ligation reactions and a control were run. Each reaction contained pUAST DNA, *crammer* DNA, 10X ligase buffer, T4 ligase, and water as summarized in Table 5. Different amounts of *crammer* DNA were used to determine the most effective reaction mixture (Table 5). The reactions were assembled in PCR tubes and a thermocycler was used to keep the mixtures at 16° C overnight.

Table 5: Ligation Reagents

	Ligation 1	Ligation 2	Ligation 3	Control
pUAST DNA (Digested with EcoR1 and Xho1)	5 μ L	5 μ L	5 μ L	5 μ L
<i>Crammer</i> DNA (Digested with EcoR1 and Xho1)	2 μ L	4 μ L	6 μ L	0 μ L
10X Buffer	1.5 μ L	1.5 μ L	1.5 μ L	1.5 μ L
10X T4 Ligase	1 μ L	1 μ L	1 μ L	1 μ L
H2O	5.5 μ L	3.5 μ L	1.5 μ L	7.5 μ L
Total	15 μL	15 μL	15 μL	15 μL

Transformation

Once the ligation was complete, DH5 α competent cells (Purchased from Invitrogen, Catalogue #18265-017) were transformed with ligation reaction mixture. The DH5 α cells were thawed on ice and 50 μ L of cells were used in each transformation reaction. The entire 15 μ L ligation reaction was added to the competent cells. This mixture was allowed to cool for 30 minutes in a 4 $^{\circ}$ C ice bath. The cells were heat shocked in a 42 $^{\circ}$ C water bath for 20s and 950 μ L of pre-warmed LB broth was added to the reactions. Transformed cells were grown in a shaking incubator for 60 minutes at 37 $^{\circ}$ C and 225 RPMs. After incubating, 250 μ L were spread on pre-warmed LB/Ampicillin (100 μ g/mL) plates and the plates were incubated 16-24h at 37 $^{\circ}$ C. Colonies were picked and allowed to grow up in 15mL LB broth overnight.

Miniprep

The QIAprep Spin Miniprep Kit (Catalogue #27104, Qiagen Inc.) was used to extract DNA from the overnight cultures and 5mL of bacteria were pelleted at 6,800xg for 3 minutes at room temperature. The pellets were re-suspended in 250µL P1 and transferred to microcentrifuge tubes. 250µL of P2 buffer was added and this reaction ran no longer than 5 minutes. 350µL of N3 Buffer was added to stop the reaction. The samples were centrifuged for 10 minutes at 17,900xg at room temperature and 800µL of the supernatant was applied to a QIAGEN spin column. These were centrifuged at 17,900xg for 1 minute and the flow-through was discarded. The samples were washed with 500µL of Buffer PB and centrifuged at 17,900xg for 1 minute before discarding the flow-through. The samples were washed with 750µL of Buffer PE and centrifuged at 17,900xg for 1 minute and the flow-through discarded. An additional centrifuge step was used to get rid of any residual buffer. The spin-column was placed in a fresh microcentrifuge tube and 50µL of Buffer EB was added to elute the DNA. This was allowed to stand for 1 minute and then centrifuged at 17,900xg for 1 minute. This final flow-through contained the extracted DNA. A Nanodrop was used to determine the DNA concentration and purity.

Sequencing

The sequencing reaction was set up according to Table 6. The *crammer* DNA was quantified by using spectrophotometry with a Nanodrop and the yield was 195.6 ng/µL. A total of six different primers were used for sequencing, three forward primers and three reverse primers (Table 7). Originally, one forward

primer and one reverse primer were used. Two additional forward internal primers and two additional reverse internal primers were later used. Once the sequencing reaction was set up with a Zymo Research Genomic DNA Clean and Concentrator Kit (Catalogue #D4011), the samples were loaded into a T100 Thermal Cycler for 35 cycles according to the program in Table 8.

Table 6: Sequencing Reaction Setup

Reagents	Amount
Sterile Water	4.5 μ L
5X Sequencing Buffer	2 μ L
BigDye v3.1 Sequencing RR-100	2 μ L
Forward or Reverse Primer (0.5 μ M)	0.5 μ L
DNA Template	1 μ L
Total	10 μL

Table 7: Sequencing Primers

Primer	Sequence
Forward	5'-ATGTCCTGGTTTCAGATGA-3'
Reverse	5'-TTAATTTGGCGGCACCTTTT-3'
Internal Forward 1	5'-TCTGATGCGTCGTAGAATCT-3'
Internal Reverse 1	5'-CCATTTTCCAAGTCACTTCG-3'
Internal Forward 2	5'-GTGACTTGGAAAATGGGAAT-3'
Internal Reverse 2	5'-TCTACGACGCATCAGATCCT-3'

Table 8: Thermal Cycler Sequencing

Step	Temperature	Time
Denature	96° C	30 Seconds
Anneal	50° C	15 Seconds
Extension	60° C	4 Minutes

Once the sequencing reaction was finished, Qiagen DyeX (Catalogue #27106) columns were used to clean up the samples. The spin columns were gently vortexed to resuspend the resin. The caps were loosened a quarter turn to avoid a vacuum and the bottom of the columns were snapped off. The DyeX columns were placed in 2mL collection tubes and centrifuged for 3 minutes at 2,300xg. After centrifugation, the spin columns were transferred to a clean centrifuge tube. The sequencing reaction was applied directly onto the center of the slanted gel bed surface. The reaction mixture and the pipet tip were not allowed to touch the sides of the column. The sample was pipetted slowly to ensure proper absorption into the gel. The columns were centrifuged for 3 minutes at 2,700xg. The spin column was discarded and the eluate saved in the microcentrifuge tube. The samples were dried in a speed-vacuum for 60 minutes with no heat and rehydrated in 20 μ L formamide buffer. The samples were loaded onto the Thermo-Fisher ABI Prism 3130 Genetic Analyzer.

3 Results

3.1 Over-expression of *cp1* leads to an increase in collagenase activity

The focus of this study was to characterize the effects of CP1 on the basement membrane within *Drosophila* wing discs as well as discovering the role that *cp1* plays within the well-conserved *wingless* signaling pathway. Previous research in the Srivastava laboratory by Qian Dong and others indicated that the overexpression of *cp1* lead to an increase of collagenase activity in the wing disc of wandering third instar larva. To quantify this activity we performed a series of collagenase assays on the *cp1* overexpression line *UAS-CP1-3XHA* crossed to *Ptc-gal4,UAS-srcRFP/CyO*. The collagenase assay was performed on 67 wing discs. We found an increase in collagenase activity compared to the wild type line (Figure 12). These results confirm previous findings from the Srivastava Lab by Qian Dong and others and quantifies the range of degradation caused by overexpression of CP1. Performing the collagenase assay on a larger number of discs increased our confidence in our results.

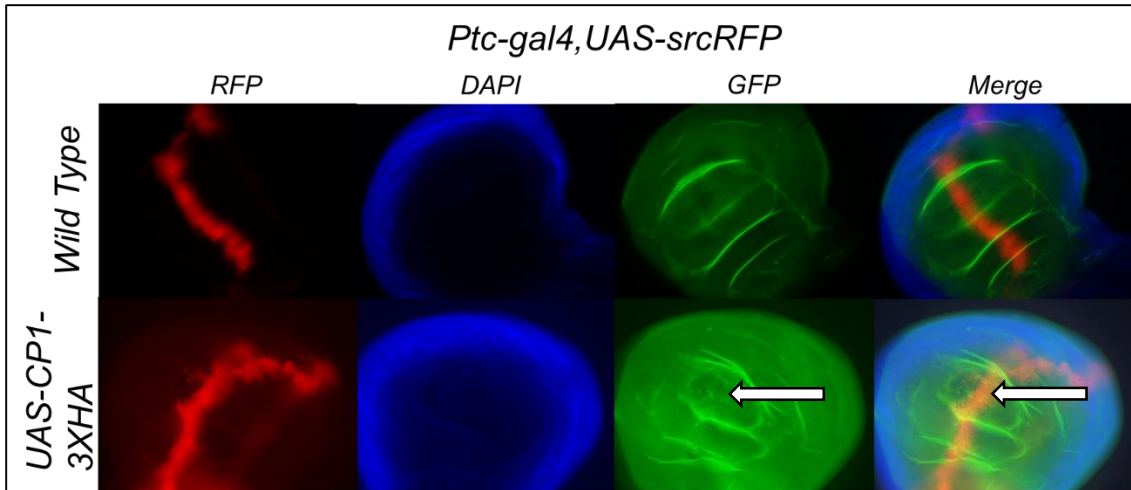


Figure 12: Collagenase Assay of *cp1* overexpression

Overexpression of *cp1* leads to upregulation of collagenase activity (green fluorescing dots) in the wing pouch along the *patched* pattern (red fluorescence). Higher collagenase activity indicates more basement membrane breakdown (arrows). The top row displays the assay in the wild type and the bottom row displays the assay with *cp1* overexpressed. Individual color channels are indicated.

3.2 Overexpression of *timp* and *cp1* mitigates effects of CP1 mediated BM degradation

We wanted to examine potential mechanisms for CP1's ability to break down the basement membrane. One hypothesis was that CP1 was utilizing MMPs breakdown collagen, as suggested by previous work in the Srivastava Laboratory. We hypothesized that if CP1 was working through MMPs, then the overexpression of *timp* should reduce the amount of collagenase activity. The *timp* suppression of basement membrane breakdown would occur because TIMPs inhibit MMPs and in this experiment would inhibit CP1 activity. To test this further, we crossed the *Drosophila* lines *UAS-CP1-3XHA* (males) and *w(UAS-TIMP, w+)/FM7* (virgin females). We then selected males from this cross and mated them with *Ptc-gal4,UAS-srcRFP/CyO* virgin females to get both *cp1* and *timp* overexpressed within the same fly line. The collagenase assays were only performed on female larvae. Figure 13 shows the different levels of collagenase activity in wing discs, from high activity (5) to no activity (0). This is an arbitrary scale based on relative signal intensity. Figure 14 shows the collagenase activity in the *cp1* overexpression line compared to the *cp1* and *timp* overexpression line. We found more wing discs in the *cp1* overexpression line with high and medium collagenase activity compared to the *cp1* and *timp* overexpression line. The *timp* and *cp1* line had 47% of discs with no collagenase activity. The *cp1* overexpression line had 12% of discs with no collagenase activity. This data supports our hypothesis that CP1 is utilizing MMPs to breakdown the BM (Figures 13 and 14).

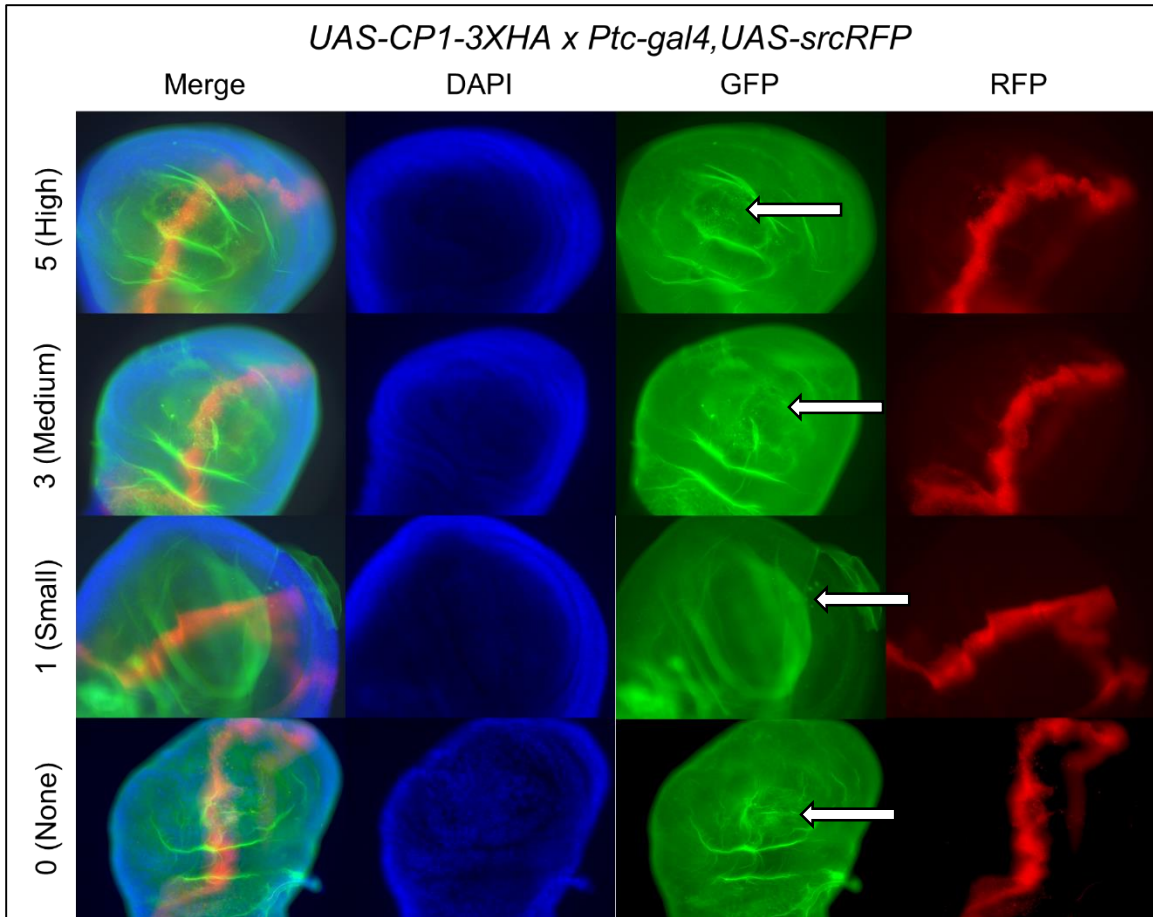


Figure 13: Examples of different collagenase activity levels

This figure demonstrates different examples we used for assigning collagenase activity levels to the wing discs after performing collagenase assays. The top row displays the highest level of collagenase activity (5) and the rows descend in severity to no activity on the bottom row (0).

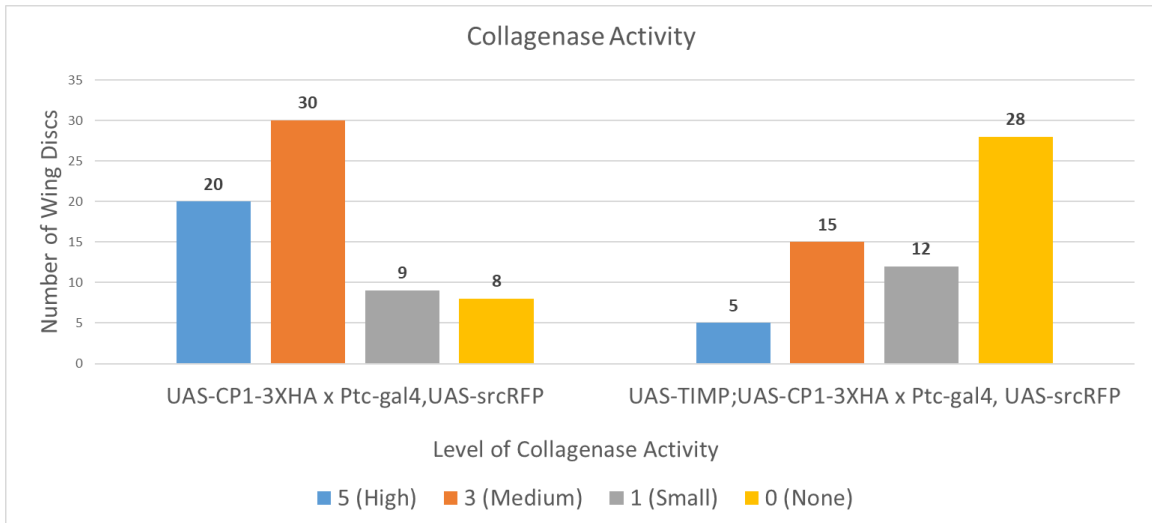


Figure 14: Different levels of collagenase activity when *cp1* is overexpressed compared to when *cp1* and *timp* are simultaneously overexpressed

Sixty-seven of the *cp1* overexpression line wing discs and 60 of the *cp1* and *timp* overexpression line wing discs were assigned collagenase activity levels with values from 0-5, with 0 indicating no activity and 5 indicating high collagenase activity. The *cp1* overexpression line had 75% of the wing discs with high and medium levels of collagenase activity. The *cp1* and *timp* overexpression line had 67% of the discs displaying small or no activity.

3.3 Downregulating *cp1* affects *wingless* signaling

To characterize *cp1* signaling in *Drosophila* wing discs, we tested the interaction between *cp1* and *wg*. A wild type line was used as a control and a *cp1* knockdown line (*UAS-CP1-RNAi/CyO; UAS-DCR2/TM₆Tb*) crossed to the *Ptc-gal4, UAS-srcRFP/CyO* line was used to look at the effects on *wg* signaling. The *wg* staining was detected using a *wg* antibody. The wild type line showed the classic expression of *wg* in the wing pouch and the surrounding inner and outer rings (Figure 15). In the *cp1* downregulation line, the *wg* signaling is interrupted within the *patched* pattern (the red line), where little to no *cp1* expression is occurring. This indicates that *wg* expression in the *Drosophila* wing hinge requires *cp1* signaling, which was a previously unexplored research area.

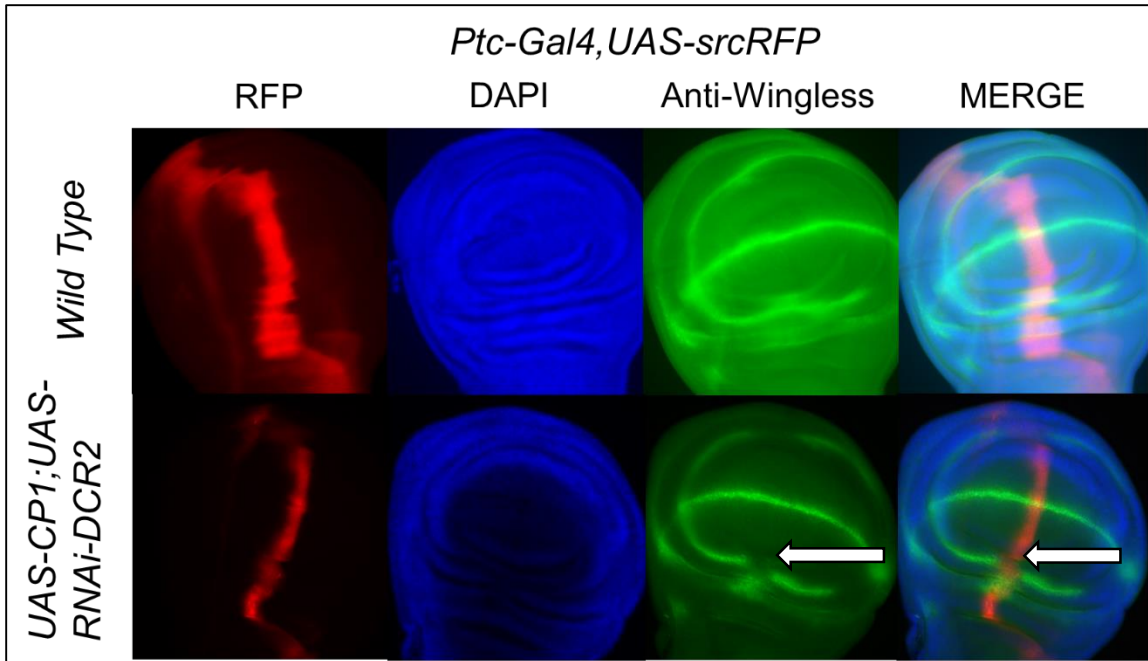


Figure 15: *Wingless* antibody staining in wild type and *cp1* downregulation wing discs

The top row shows the antibody staining in wing discs derived from wild type flies. The expression of *wg* matches up with previous results showing normal *wg* signaling (DEL ÁLAMO RODRÍGUEZ 2002). The bottom row demonstrates that *wg* signaling is interrupted within the red *patched* pattern where *cp1* is downregulated.

3.4 Downregulating *cp1* affects *nubbin* signaling

Once we demonstrated that knocking out *cp1* affects *wg* signaling, we wanted to determine *cp1*'s role with other genes in the *wingless* signaling pathway. One gene that *wg* signaling affects is *nubbin*. We performed a *nub* antibody staining with wild type flies as the control and another staining with *cp1* knocked out. *cp1* was once again knocked out throughout the *patched* pattern and the wing discs were stained for *nub* expression. The staining in wild type flies shows relatively uniform expression of *nub* throughout the wing pouch. As expected, distinct lines can be noted at the inner and outer rings as well as the wing margin through the center (Figure 16). The *nub* antibody staining with *cp1* downregulation flies reveals a loss of *nub* expression throughout nearly the entire *patched* pattern. The loss of *nub* expression can be seen at the inner and outer rings of the wing blade. There also appears to be less expression through the center of the wing pouch, including the wing margin (Figure 16).

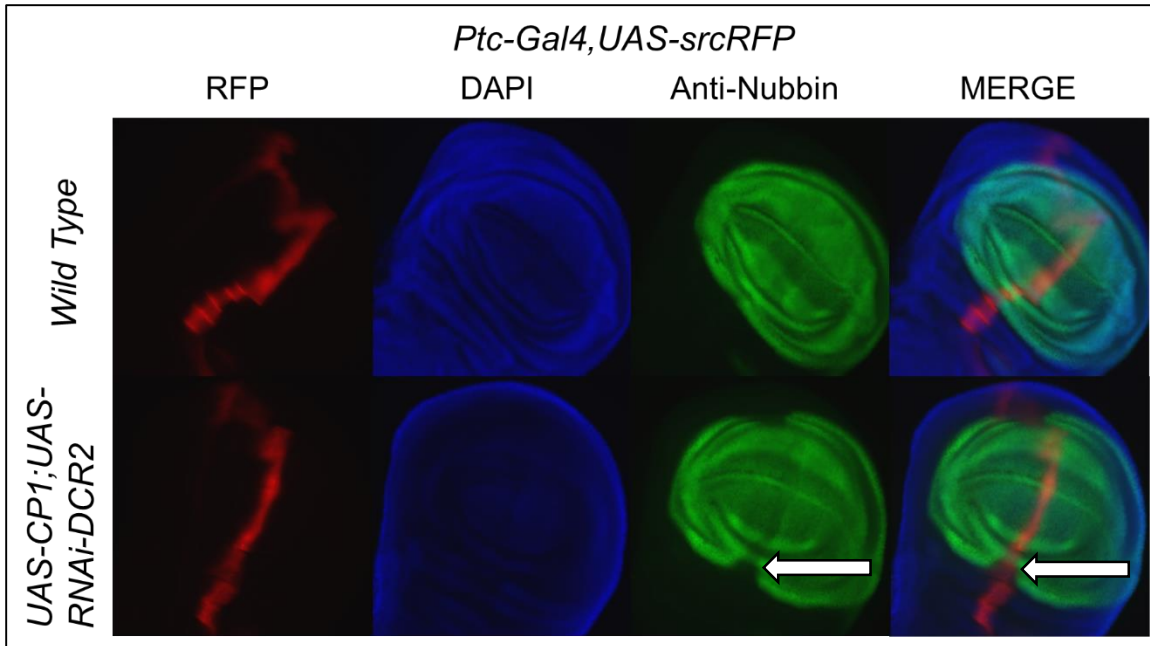


Figure 16: *Nubbin* antibody staining in wild type and *cp1* downregulation wing discs

The top row shows the *nub* antibody staining in wild type flies. The expression of *nub* matches up with previous research showing normal *nub* signaling. The bottom row demonstrates that *nub* signaling is interrupted within the red *patched* pattern where *cp1* is knocked out.

3.5 Downregulating *cp1* does not affect *vestigial* signaling

Vg is another important gene within the *wg* signaling pathway. *Vg* is upstream to *wg* signaling in early hinge development. Previous research has demonstrated that expression of *wg*, *rn*, and *nub* requires *vg*. Determining if *cp1* expression affects *vg* signaling provides a clearer picture of *cp1*'s overall effects. Figure 17 shows that a downregulation of *cp1* does not affect *vg* expression.

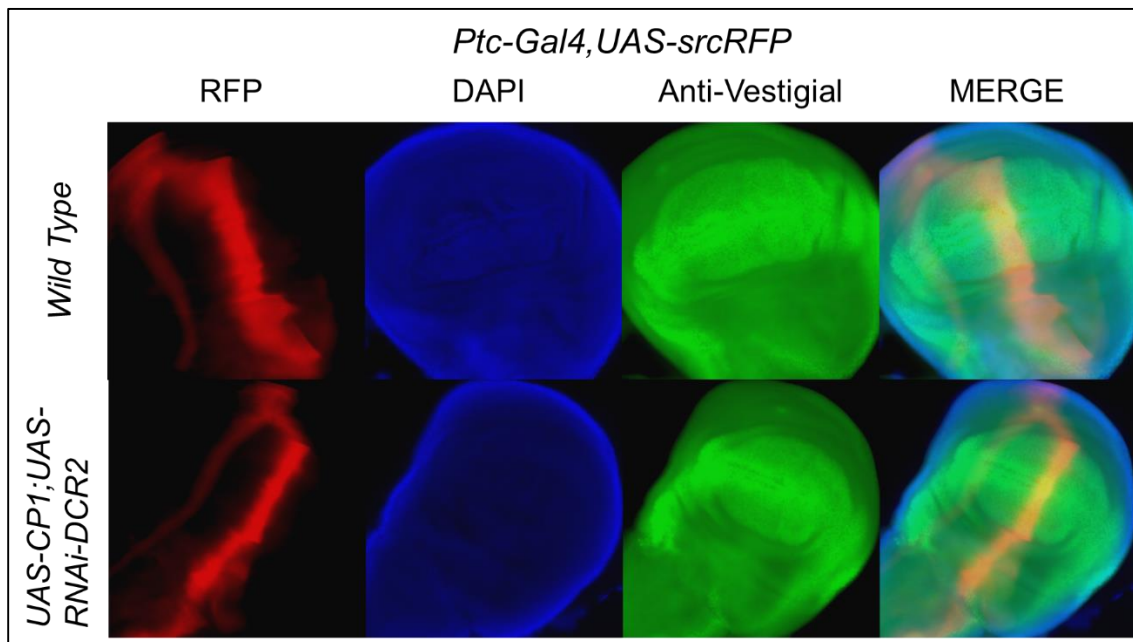


Figure 17: *Vestigial* antibody staining in wild type and *cp1* downregulation wing discs shows that *vg* is unaffected.

The top row shows the *vg* antibody staining in wild type flies. The expression of *vg* matches up with previous research showing normal *nub* signaling (DEL ÁLAMO RODRÍGUEZ 2002). The bottom row demonstrates that *vg* signaling is not interrupted within the red *patched* pattern where *cp1* is knocked out.

3.6 Successful cloning and verification of the *crammer* cDNA into the vector pUAST

Although *crammer* proteins have been examined *in vitro*, we wanted to manipulate *crammer* expression *in vivo*. To investigate the effects of *crammer* with *cp1*, we cloned the *crammer* sequence into a plasmid to create transgenic *Drosophila*. The *crammer* sequence was digested out of a pUCIDT-AMP : CramEcoXho plasmid with restriction enzymes EcoR1 and Xho1. The pUAST plasmid was also digested with EcoR1 and Xho1. Figure 18 shows that the pUAST was cut and Figure 19 shows that the *crammer* sequence was cut out of the pUCIDT plasmid. The *crammer* segment can be seen at the bottom of the gel between 200-300 bp. This is appropriate because the *crammer* coding sequence is 240 bp.

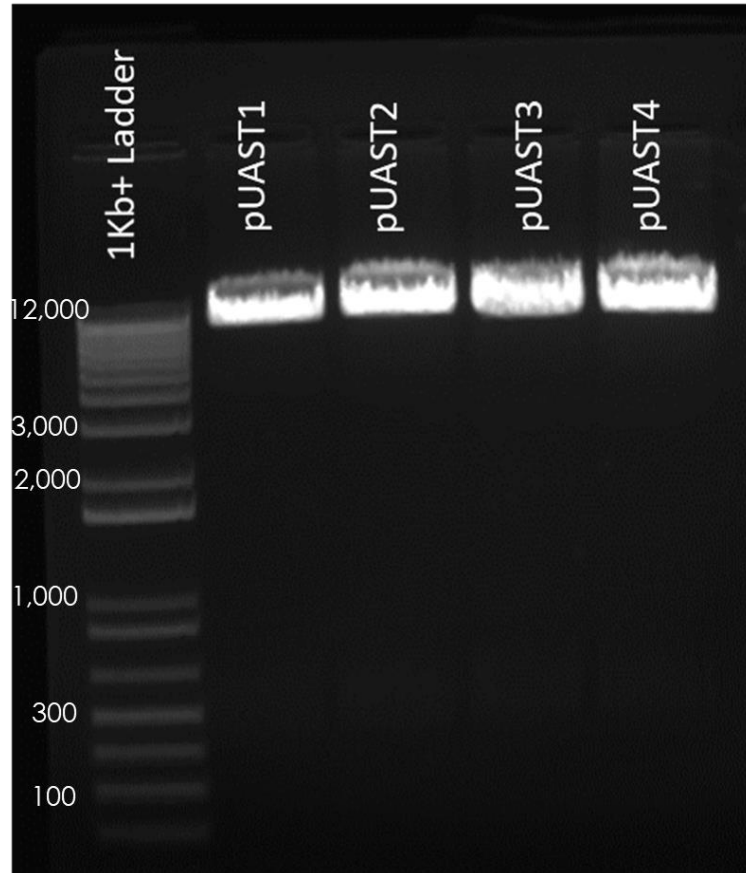


Figure 18: pUAST digestion with EcoR1 and Xho1 (1% Gel)

The plasmid has been digested for 2.5 hours and is open and ready to be ligated with the *crammer* sequence. A 1Kb+ ladder (LifeTech/Invitrogen) was used.

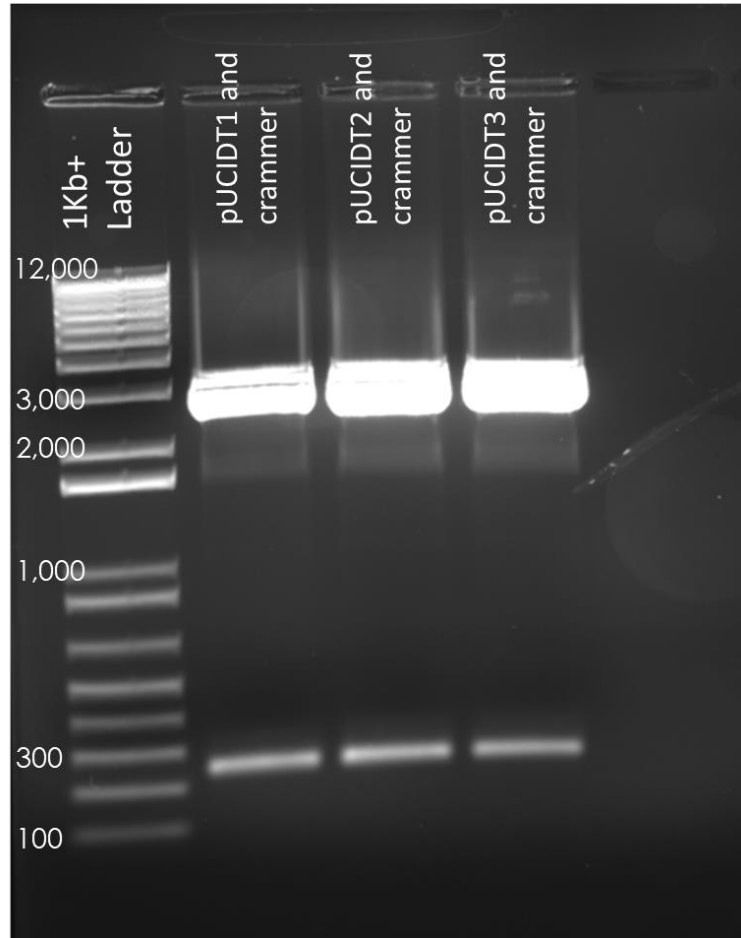


Figure 19: pUCIDT-AMP : CramEcoXho with EcoR1 and Xho1 (1% Gel)

The plasmid has been digested and the crammer sequence is clearly visible between the 200-300bp markers of the 1Kb+ Ladder (LifeTech/Invitrogen).

After the pUAST and *crammer* DNA were gel extracted, they were ligated together overnight and transformed into DH5 α *E. coli*. Each transformation plate had >100 colonies. Colonies were picked and allowed to grow in LB Broth overnight before the DNA was extracted. This DNA was digested to check that the pUAST plasmid contained the *crammer* sequence. Figure 20 shows that the pUAST had a new sequence inserted, and a sequencing reaction was performed to ensure that the *crammer* sequence was accurate. The sequencing traces are provided in the appendix.

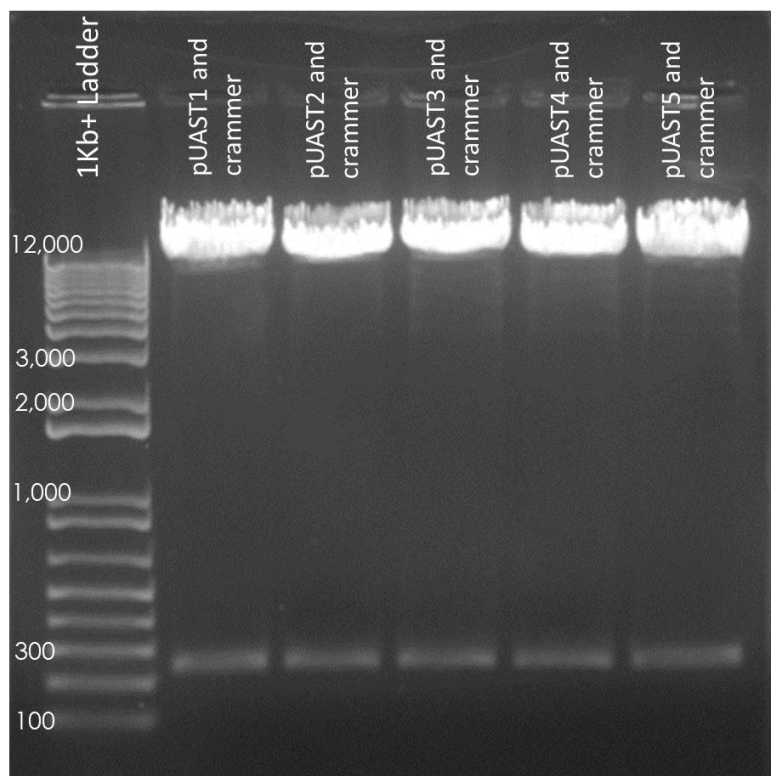


Figure 20: pUAST with release of *crammer* gene upon digestion with EcoR1 and Xho1 (1% Gel)

This displays the pUAST plasmid after ligation with the *crammer* sequence. The plasmid was digested with EcoR1 and Xho1. The *crammer* sequence can be seen between the 200 and 300bp markers of the 1Kb+ Ladder (LifeTech/Invitrogen).

4 Discussion and Future Directions

Our study quantified the collagenase activity of CP1 as well as a possible mechanism for BM degradation via MMPs. Previous research by Qian Dong and others demonstrated that CP1 is expressed in air sac primordia and wing discs and has the ability to degrade the ECM (DONG ET AL 2015). Knowing that the overexpression of CP1 leads to greater collagenase activity in wing discs, we originally hypothesized that CP1 was working through MMPs and thus resulting in BM degradation. Because TIMPs inhibit MMPs, we wanted to examine the effects of overexpressing both CP1 and TIMP on collagenase activity. We reasoned that if CP1 is working through MMPs in some manner, then the overexpression of TIMP would lead to a decrease of collagenase activity in the W(UAS-TIMP, w+)/FM7; Ptc-gal4,UAS-srcRFP; UAS-CP1-3XHA double expression line. This study showed various levels of collagenase activity when CP1 is overexpressed and that collagenase activity decreases when CP1 and TIMP are both overexpressed (Figure 14). Our results indicate that CP1 is utilizing MMPs and resulting in collagenase activity and BM degradation. CP1 may be acting as an upstream regulator on MMPs, controlling expression and activity within the wing pouch. However, this needs to be experimentally verified.

Understanding the scope and mechanisms of CP1's ability to degrade the ECM is important because of its relation to cancer metastasis. Cancerous tumors metastasize to other organs in the body and this occurrence is dependent on angiogenesis. The formation of new blood vessels for a tumor requires breakdown of surrounding basement membrane, which contains collagen. As

shown in Table 1, the Cathepsin L protein has been associated with cancer in several model organisms. Characterizing CP1 will allow for greater insight into cancerous mechanisms. The relationship between CP1 and cancer in *Drosophila* may be examined by inducing tumors in fruit flies (SRIVASTAVA 2013). The levels of CP1 expression within tumors or the levels of collagenase activity due to CP1 activity around metastasizing cells may help determine CP1's role in cancer growth.

A previously unexplored area of research was the potential communication between CP1 and genes within the *wingless* signaling pathway. This signaling pathway is important to study in relation to CP1 because *wg* is a Wnt homologue in *Drosophila*. The Wnt signaling pathway is an evolutionarily conserved cell signaling pathway that regulates development throughout embryogenesis and adult homeostasis. We demonstrated with a series of antibody stains that CP1 signaling affects *wg* and *nub*, but does not affect *vg* (Figures 15, 16, and 17). All of these characterizations are important by helping us understand where CP1 fits within the *wg* pathway (Figure 21). *Vg* is known to be upstream of *wg* and *nub*, and *vg* expression is required for proper expression of these genes. A null allele of *vg* results in no expression of *wg*, *nub*, and *rn* in the wing pouch (DEL ÁLAMO RODRÍGUEZ 2002).

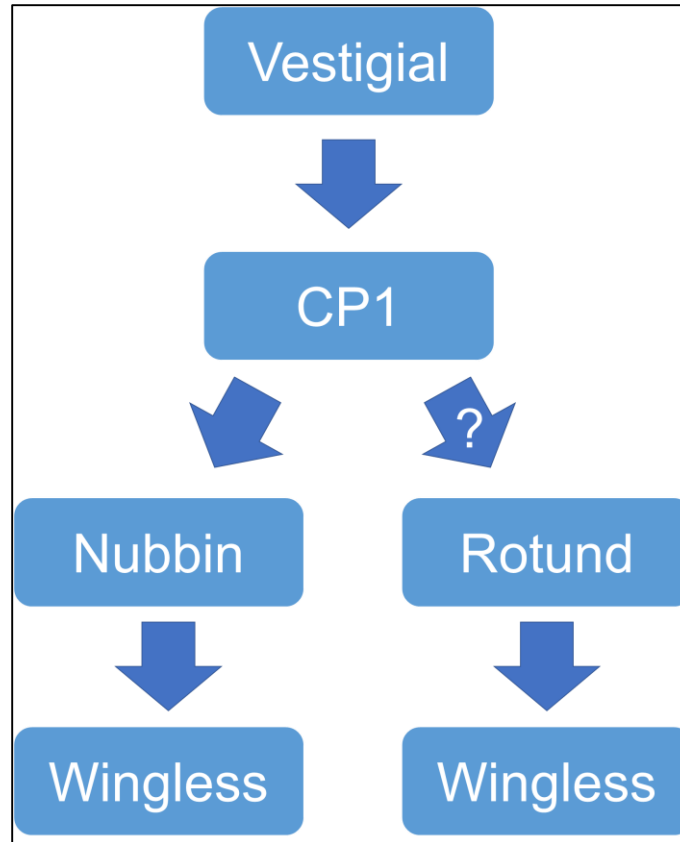


Figure 21: Potential new placement of CP1 within the wingless signaling pathway. Our results demonstrate that CP1 is acting as an upstream regulator of *nub*, *wg*, and potentially *rn*. *Vg* appears to be upstream of all genes we studied.

The antibody stains demonstrating the effects of CP1 downregulation helps begin the process of placing this cathepsin in the *wingless* signaling pathway (Figure 21). These stains also demonstrate that CP1 is acting as an upstream regulator within the *wingless* pathway. One example of studying CP1 as an upstream regulator is performing an antibody stain of *rn* with CP1 downregulated. *Rn* expression requires *vg* and an antibody stain could potentially determine if CP1 expression is required as well. Because CP1 downregulation

did not affect *vg* expression but did interfere with *wg* and *nub*, we would expect *rn* to be affected as well.

The cloning of *crammer* into a vector will enable more avenues for exploring the relationship between *crammer* and CP1. *Crammer* has been shown to be an inhibitor of cathepsins *in vitro* (DESHAPRIYA 2007), and demonstrating this effect in a model organism has the potential to solidify the hypothesis that *crammer* functions as a selective inhibitor. The PUASt vector with the *crammer* insert has been sent to a private company in order to generate transgenic flies so that *in vivo* studies are possible. With the development of these transgenic flies, *crammer* can be overexpressed in combination with CP1 or downregulated much as CP1 has been in this research. The overexpression of *crammer* may affect CP1's ability to degrade the ECM, and we will be able to compare collagenase assays of larvae with *crammer* overexpressed to larvae with CP1 overexpressed. The downregulation of *crammer* may have the opposite effect. These future results with *crammer* can be compared with the chart in Figure 13 to compare different levels of collagenase activity in different conditions.

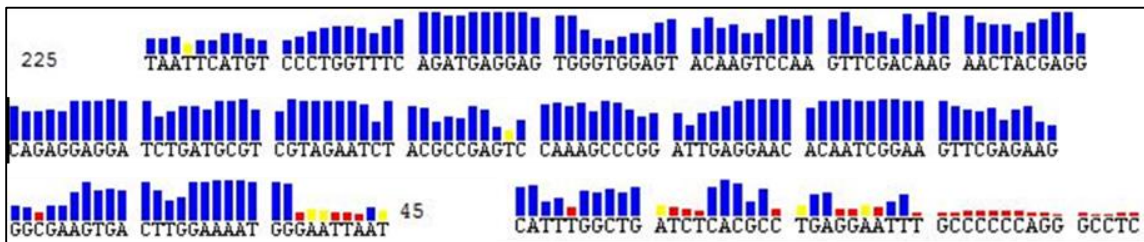
We would also like to explore an RNA in situ hybridization with a *crammer* probe. Previous research in the Srivastava laboratory has demonstrated the results of a RNA in situ hybridization with a CP1 probe. With hybridization results from *crammer* and CP1 probes, the localization of both genes' mRNA can be examined. Because *crammer* has only been shown as an inhibitor of CP1 *in vitro*, the data from these two hybridization probes could help elucidate whether the mRNA localizes to similar or disparate areas within *Drosophila* wing discs.

This study has helped quantify CP1's ability to degrade the BM and its potential mechanism via MMPs. The antibody stainings with *wg*, *vg*, and *nub* are novel experiments and will help place *cp1* within the *wg* signaling pathway once additional genes are tested. The cloning of *crammer* into a plasmid to create transgenic flies will allow for *in vivo* experimentation of this potential inhibitor. We have characterized several aspects of CP1 activity but there is still much work that needs to be done to better understand its role in BM degradation and signaling.

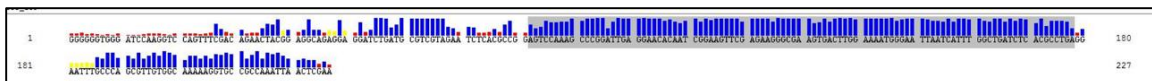
Appendix

As mentioned previously, we utilized six primers to sequence the *crammer* cDNA sequence that was inserted into the pUAST. We compiled three different sequencing runs to confirm that the *crammer* cDNA was accurate. Blue bases indicate high confidence, yellow indicates medium confidence, and red indicates low confidence. The first image of this appendix is the sequencing run with the *crammer* reverse primer (reverse complemented). From the results, we had high confidence that bases 1-146 were accurate. The second image shows the *crammer* forward primer and we had high confidence that bases 102-197 were accurate. The third image is an internal forward primer that started pairing at base 75. From the sequencing run, this result gave us high confidence that bases 179-240 were accurate. Overall, we determined with high confidence that the *crammer* cDNA's 240 bases were accurate.

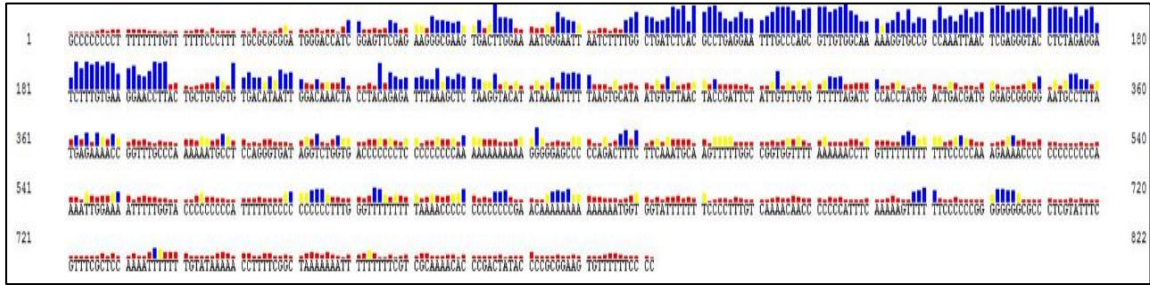
Crammer Reverse Primer (Reverse Complemented) (Bases 1-146)



Crammer Forward Primer (Bases 102-197)



Cramer Forward Primer 1 (Bases 179-240)



References

- Alberts, B., 2017 Molecular biology of the cell. Garland Science. 1036
- Bejsovec, A., 2013 *Wingless/Wnt* signaling in *Drosophila*: the pattern and the pathway. *Molecular reproduction and development* 80: 882-894.
- Brand, Andrea H., and Norbert Perrimon, 1993 Targeted gene expression as a means of altering cell fates and generating dominant phenotypes. *Development* 118: 401-415.
- Brindle, N. R., et al, 2015 Deficiency for the cysteine protease cathepsin L impairs Myc-induced tumorigenesis in a mouse model of pancreatic neuroendocrine cancer. *PloS one* 10.
- Britton, C., and Linda Murray, 2002 A cathepsin L protease essential for *Caenorhabditis elegans* embryogenesis is functionally conserved in parasitic nematodes. *Molecular and biochemical parasitology* 122: 21-33.
- Cawston, T. E., and David A. Young, 2010 Proteinases involved in matrix turnover during cartilage and bone breakdown. *Cell and tissue research* 339: 221-235.
- Čeru, S., et al, 2010 Stefin B interacts with histones and cathepsin L in the nucleus. *Journal of Biological Chemistry* 285: 10078-10086.
- Chauhan, S. S., Lori J. Goldstein, and Michael M. Gottesman, 1991 Expression of cathepsin L in human tumors. *Cancer research* 51: 1478-1481.
- Chauhan, S. S., Popescu, N. C., Ray, D., Fleischmann, R., Gottesman, M. M., & Troen, B. R., 1993 Cloning, genomic organization, and chromosomal localization of human cathepsin L. *Journal of Biological Chemistry* 268: 1039-1045.
- Cheng, T., et al, 2006 Cystatin M/E Is a High Affinity Inhibitor of Cathepsin V and Cathepsin L by a Reactive Site That Is Distinct from the Legumain-binding Site A NOVEL CLUE FOR THE ROLE OF CYSTATIN M/E IN EPIDERMAL CORNIFICATION. *Journal of Biological Chemistry* 281: 15893-15899.
- Dantoft, W., et al, 2013 The Oct1 homolog Nubbin is a repressor of NF- κ B-dependent immune gene expression that increases the tolerance to gut microbiota. *BMC biology* 11: 99.
- Davies, D. R., 1990 The structure and function of the aspartic proteinases. *Annual review of biophysics and biophysical chemistry* 19: 189-215.
- del Álamo Rodríguez, D., et al, 2002 Different mechanisms initiate and maintain wingless expression in the *Drosophila* wing hinge. *Development* 129: 3995-4004.
- Delbridge, M. L., and Leonard E. Kelly, 1990 Sequence analysis, and chromosomal localization of a gene encoding a cystatin-like protein from *Drosophila melanogaster*. *FEBS letters* 274: 141-145.
- Dennemärker, J., et al, 2010 Deficiency for the cysteine protease cathepsin L promotes tumor progression in mouse epidermis. *Oncogene* 29: 1611-1621.

- Deshapriya, R. M., et al, 2007 Drosophila CTLA-2-like protein (D/CTLA-2) inhibits cysteine proteinase 1 (CP1), a cathepsin L-like enzyme. *Zoological science* 24: 21-30.
- Dong, Q., et al, 2015 A Cathepsin- L is required for invasive behavior during Air Sac Primordium development in Drosophila melanogaster. *FEBS letters* 589: 3090-3097.
- Duffy, J. B., 2002 GAL4 system in Drosophila: a fly geneticist's Swiss army knife. *genesis* 34: 1-15.
- Duong, L. T., 2012 Therapeutic inhibition of cathepsin K [mdash] reducing bone resorption while maintaining bone formation. *BoneKEy reports* 1.
- Frantz, C., Kathleen M. Stewart, and Valerie M. Weaver, 2010 The extracellular matrix at a glance. *J Cell Sci* 123: 4195-4200.
- Glasheen, B. M., et al, 2010 A matrix metalloproteinase mediates airway remodeling in Drosophila. *Developmental biology* 344: 772-783.
- Hashmi, S., et al, 2002 Cathepsin L is essential for embryogenesis and development of *Caenorhabditis elegans*. *Journal of Biological Chemistry* 277: 3477-3486.
- Hays, R., Gil B. Gibori, and Amy Bejsovec, 1997 *Wingless* signaling generates pattern through two distinct mechanisms. *Developmental biology* 124: 3727-3736.
- Henriet, P., Laurence Blavier, and Yves A. Declerck, 1999 Tissue inhibitors of metalloproteinases (TIMP) in invasion and proliferation. *Apmis* 107: 111-119.
- Ignotz, R. A., and Joan Massague, 1986 Transforming growth factor-beta stimulates the expression of fibronectin and collagen and their incorporation into the extracellular matrix. *Journal of Biological Chemistry* 261: 4337-4345.
- LeBleu, V. S., Brian MacDonald, and Raghu Kalluri, 2007 Structure and function of basement membranes. *Experimental biology and medicine* 232: 1121-1129.
- Li, A. C. Y., and R. P. H. Thompson, 2003 Basement membrane components. *Journal of Clinical Pathology*: 885-887.
- Liotta, L. A., 1986 Tumor invasion and metastases—role of the extracellular matrix: Rhoads Memorial Award lecture. *Cancer research* 46: 1-7.
- Lyons, G. R., et al, 2014 Cysteine proteinase-1 and cut protein isoform control dendritic innervation of two distinct sensory fields by a single neuron. *Cell reports* 6: 783-791.
- Matsumoto, I., et al, 1995 A putative digestive cysteine proteinase from Drosophila melanogaster is predominantly expressed in the embryonic and larval midgut. *The FEBS Journal* 227: 582-587.
- Matta, B.P., Bitner-Mathé, B.C. & Alves-Ferreira, M, 2011 Getting real with real-time qPCR: a case study of reference gene selection for morphological variation in Drosophila melanogaster wings. *Dev Genes Evol* 221: 49.

- Neumann, C. J. a. C., S. M, 1996 Distinct mitogenic and cell fate specification functions of *wingless* in different regions of the wing. *Developmental biology* 122: 1781-1789.
- Nga, B. T., et al, 2014 Studies of inhibitory mechanisms of propeptide-like cysteine protease inhibitors. *Enzyme research*.
- Page-McCaw, A., et al, 2003 Drosophila matrix metalloproteinases are required for tissue remodeling, but not embryonic development. *Developmental cell* 4: 95-106.
- Rawlings, N. D., Alan J. Barrett, and Alex Bateman, 2010 MEROPS: the peptidase database. *Nucleic acids research* 38: D227-D233.
- Reiter, L. T., Potocki, L., Chien, S., Gribskov, M., & Bier, E, 2001 A systematic analysis of human disease-associated gene sequences in Drosophila melanogaster. *Genome research* 11: 1114-1125.
- Schauer, S., T. Burster, and M. Spindler- Barth, 2012 N- and C- terminal degradation of ecdysteroid receptor isoforms, when transiently expressed in mammalian CHO cells, is regulated by the proteasome and cysteine and threonine proteases. *Insect molecular biology* 21: 383-394.
- Skeath, J. B., 1999 At the nexus between pattern formation and cell- type specification: the generation of individual neuroblast fates in the Drosophila embryonic central nervous system. *Bioessays* 21: 922-931.
- Smith, H. W., and Chris J. Marshall, 2010 Regulation of cell signalling by uPAR. *Nature reviews Molecular cell biology* 11: 23-36.
- Srivastava, A., et al, 2007 Basement membrane remodeling is essential for Drosophila disc eversion and tumor invasion. *Proceedings of the National Academy of Sciences* 104: 2721-2726.
- Srivastava, A, 2013 A protocol for genetic induction and visualization of benign and invasive tumors in cephalic complexes of Drosophila melanogaster. *JoVE* 79.
- Sudhan, D. R., and Dietmar W. Siemann, 2015 Cathepsin L targeting in cancer treatment. *Pharmacology & therapeutics* 155 105-116.
- Sudhan, D. R., et al, 2016 Cathepsin L in tumor angiogenesis and its therapeutic intervention by the small molecule inhibitor KGP94. *Clinical & experimental metastasis* 33: 461-473.
- Swarup, S., and Esther M. Verheyen, 2012 Wnt/wingless signaling in Drosophila. *Cold Spring Harbor perspectives in biology* 4.
- Tingaud-Sequeira, A., and Joan Cerdà, 2007 Phylogenetic relationships and gene expression pattern of three different cathepsin L (Ctsl) isoforms in zebrafish: Ctsla is the putative yolk processing enzyme. *Gene* 386: 98-106.
- Tryselius, Y., and D. Hultmark, 1997 Cysteine proteinase 1 (CP1), a cathepsin L- like enzyme expressed in the Drosophila melanogaster haemocyte cell line mbn- 2. *Insect molecular biology* 6: 173-181.
- Tseng, T.-S., et al, 2012 A molten globule-to-ordered structure transition of Drosophila melanogaster crammer is required for its ability to inhibit cathepsin. *Biochemical Journal* 442: 563-572.

- Turk, V., et al, 2012 Cysteine cathepsins: from structure, function and regulation to new frontiers. *Biochimica et Biophysica Acta (BBA)-Proteins and Proteomics* 1824: 68-88.
- Vierstraete, E., Anja Cerstiaens, Geert Baggerman, Gert Van den Bergh, Arnold De Loof, and Liliane Schoofs, 2003 Proteomics in *Drosophila melanogaster*: first 2D database of larval hemolymph proteins. *Biochemical and biophysical research communications* 304): 831-838.
- Visse, R., and Hideaki Nagase, 2003 Matrix metalloproteinases and tissue inhibitors of metalloproteinases structure, function, and biochemistry. *Circulation research* 92: 827-839.
- Wu, X., Krista Golden, and Rolf Bodmer, 1995 Heart development in *Drosophila* requires the segment polarity gene *wingless*. *Developmental biology* 169: 619-628.